

The production and decay of $X_0(2900)$ state with different interpretation

Zi-Yan Yang^{1,2}, Qian Wang^{1,2,4,*} and Wei Chen^{3,4,†}

¹Key Laboratory of Atomic and Subatomic Structure and Quantum Control (MOE),
Guangdong Basic Research Center of Excellence for Structure and Fundamental Interactions of Matter,
Institute of Quantum Matter, South China Normal University, Guangzhou 510006, China

²Guangdong-Hong Kong Joint Laboratory of Quantum Matter,
Guangdong Provincial Key Laboratory of Nuclear Science, Southern Nuclear Science Computing Center,
South China Normal University, Guangzhou 510006, China

³School of Physics, Sun Yat-sen University, Guangzhou 510275, China and

⁴Southern Center for Nuclear-Science Theory (SCNT), Institute of Modern Physics,
Chinese Academy of Sciences, Huizhou 516000, Guangdong Province, China

The observation of $X_0(2900)$ in $B^+ \rightarrow D^+ D^- K^+$ decay process indicates the existence of open flavor tetraquark states. We study the production and decay of $X_0(2900)$ state with final state interaction mechanism, where we calculate the strong vertices such as $g_{\bar{D}KX_0}$, $g_{\bar{D}^*K^*X_0}$, $g_{D_s^+ \bar{D}K}$ and $g_{D_{s1} \bar{D}K^*}$ in the framework of QCD sum rules method. We find that for the interpretation of the $\bar{D}^* K^*$ molecule of $X_0(2900)$, the branching fraction of the production process and the decay width are consistent with the experimental results, indicating that the observed $X_0(2900)$ could be interpreted as the $\bar{D}^* K^*$ molecule. However, we cannot exclude the possibility of a compact tetraquark interpretation within the uncertainty. More experimental and theoretical efforts are needed to fully understand the nature of the $X_0(2900)$ state.

PACS numbers: 12.39.Mk, 12.38.Lg, 14.40.Ev, 14.40.Rt

Keywords: Tetraquark states, exotic states, hadron production, QCD sum rules

I. INTRODUCTION

The study of multiquarks goes back to half a century after the quark model proposed in 1964 [1, 2] and becomes a hot topic since the observation of the $X(3872)$ in 2003. Due to the sufficient statistic in experiment, tens of charmonium-like and bottomonium-like states are observed by various experimental collaborations [3]. These hidden-charm(bottom) states could be beyond the conventional quark model and be viewed as exotic candidates. They also provide a novel platform to shed light on the hadronization mechanism. Although numerous theoretical efforts have been put forward to understand their nature [4–16], it is still unclear about the hadronization mechanism.

Besides of the hidden-flavor structure, the exotic states can be composed of quarks with fully open flavors. The first fully open flavors tetraquark candidate was observed in 2016. The D0 collaboration observed a narrow structure $X(5568)$ in the $B_s^0 \pi^\pm$ invariant mass spectrum with a 5.1σ significance. $X(5568)$ could be interpreted as the $sud\bar{b}$ or $s\bar{d}u\bar{b}$ tetraquark state due to the $B_s^0 \pi^\pm$ decay mode [17]. However, it was not confirmed by the LHCb [18], CMS [19], CDF [20] and ATLAS [21] collaborations. In 2020, the LHCb collaboration reported the observation of two new states $X_0(2900)$ and $X_1(2900)$ in the $D^- K^+$ invariant mass spectrum of the decay process $B^+ \rightarrow D^+ D^- K^+$ [22, 23]. The resonance parameters of these two new states are

$$\begin{aligned} X_0(2900) : m &= 2866 \pm 7 \pm 2 \text{ MeV}, \\ \Gamma &= 57 \pm 12 \pm 4 \text{ MeV}, \end{aligned} \quad (1)$$

and

$$\begin{aligned} X_1(2900) : m &= 2904 \pm 5 \pm 1 \text{ MeV}, \\ \Gamma &= 110 \pm 11 \pm 4 \text{ MeV}, \end{aligned} \quad (2)$$

respectively. The fit fraction of $X_0(2900)$ in the process $B^+ \rightarrow D^+ D^- K^+$ is measured to be $(5.6 \pm 1.4 \pm 0.5)\%$ and the branching fraction is $(2.2 \pm 0.7) \times 10^{-4}$. Thus the branching fraction of the two body cascade decay process $B^+ \rightarrow D^+ X_0(2900) \rightarrow D^+ D^- K^+$ is measured to be $(1.2 \pm 0.5) \times 10^{-5}$. Considering the isospin symmetry, one can approximately conclude that [24]

$$\mathcal{B}(B^+ \rightarrow D^+ X_0(2900)) \sim (2.4 \pm 1.0) \times 10^{-5}. \quad (3)$$

*Electronic address: qianwang@m.scnu.edu.cn

†Electronic address: chenwei29@mail.sysu.edu.cn

Since they were observed in $D^- K^+$ channel, the minimal quark contents of these states should be $\bar{c}\bar{s}du$. Thus $X_{0,1}(2900)$ could be the strong candidates of fully open flavor tetraquark states and inspired theorists' extensive interest.

Several studies indicate that $X_0(2900)$ state can be interpreted as S -wave $ud\bar{s}\bar{c}$ compact tetraquark state with different methods, such as chromomagnetic interaction model [25–27], solving Schrödinger equation with variational method [28] and QCD sum rule [29, 30]. However, some theoretical studies give a negative results for the compact tetraquark interpretations of $X_0(2900)$, for example the extended relativized quark model [31]. In Ref.[32], the authors revisit the result of Ref.[30] and consider the decay properties in the framework of the light-cone sum rule. Their results disagree with the tetraquark interpretation for $X_0(2900)$. There are also some studies prefer the $\bar{D}^* K^*$ molecular interpretation for $X_0(2900)$ because its mass is very close to the threshold of $\bar{D}^* K^*$, such as the Lippmann-Schwinger equation with leading order contact potentials [33], the Bethe-Salpeter framework [34, 35], one-boson exchange model [36], coupled-channel formalism [37] and QCD sum rule [38–41]. Even before the observation of the $X_0(2900)$, the $\bar{D}^* K^*$ molecular interpretation was investigated within hidden local gauge symmetry [42] and the predicted mass was slightly lower than the observed one. The updated analysis within the same framework can be found in Ref. [43].

Several theoretical studies consider the decay and production properties of $X_0(2900)$ [24, 44–49], which may be very sensitive to its inner structures of the multi-quark system. In Ref.[44], the authors consider the two-body strong decays into $D^- K^+$ via triangle diagrams and three-body decays into $D^* \bar{K} \pi$ assuming that $X_0(2900)$ state is a bound state of $\bar{D}^* K^*$. They conclude that the $X_0(2900)$ may have a large $\bar{D}^* K^*$ component with a non-negligible compact tetraquark component. In Refs.[46, 47], the authors make predictions for the production and decays of $X_0(2900)$ by modeling the production amplitude as a triangle diagram with non-perturbative final state interaction, and perturbative quark exchange, pion exchange and other effective field theory interactions. Their result shows that the triangle diagrams would also produce the $X_0(2900)$ signals, indicated that $X_0(2900)$ can be interpreted as a kinematic cusp effect arising from $\bar{D}^* K^*$ and $\bar{D}_1 K^{(*)}$ interactions. Meanwhile, they do not exclude the resonance scenario. In Refs.[24, 48], the authors reproduce the branching fractions of $B^+ \rightarrow D^+ X_0$ via the rescattering mechanism.

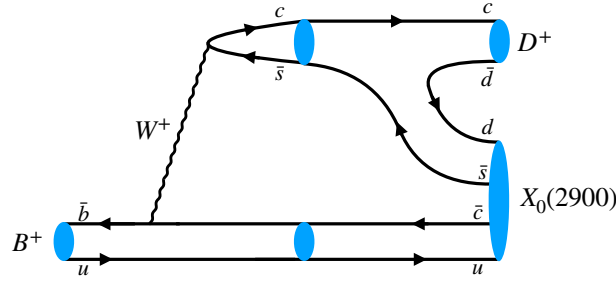


FIG. 1: Diagram contributing to $B^+ \rightarrow D^+ X_0(2900)$ at the quark level.

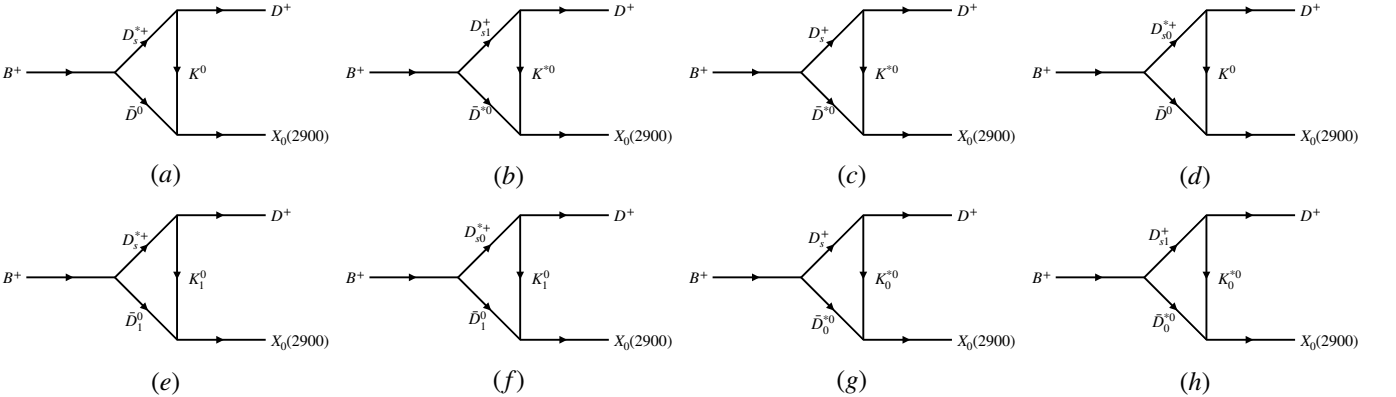


FIG. 2: Diagram contributing to $B^+ \rightarrow D^+ X_0(2900)$ at the hadron level.

At the quark level, the diagram for the process $B^+ \rightarrow D^+ X_0(2900)$ is shown in Fig. 1. The weak decay arises from a Cabibbo-favored weak transition $\bar{b} \rightarrow \bar{c}(c\bar{s})$ along with the creation of a $d\bar{d}$ pair from the strong interaction. This diagram is the so-called external W emission diagram and it is not factorizable since the weak interaction produced $c\bar{s}$ enters into different final states. Thus, long-distance contributions would play a significant role in the $B^+ \rightarrow D^+ X_0(2900)$ process, where the weak interaction produced $c\bar{s}$ hadronize as $D_{s(1)}^{(*)+}$ and $u\bar{c}$ pair hadronize as $\bar{D}^{(*)0}$, followed by the strong rescattering in D^+ and $X_0(2900)$ with K^0

meson exchange, which is the process mainly concerned in [48]. Meanwhile in Ref.[24], the authors consider the rescattering process $D_{s1}^+ \bar{D}^{*0} \rightarrow D^+ X_0(2900)$ with K^{*0} meson exchange due to the fact that $X_0(2900)$ could be a good candidate for the $\bar{D}^* K^*$ molecule and mainly decays into $\bar{D} K$. The above two rescattering processes are shown in Fig.2(a-b). Moreover, there should be other rescattering processes, such as $B \rightarrow D^* D_s \rightarrow D^+ X_0(2900)$ with K^* meson exchange. The other possible rescattering processes are shown in Fig.2(c-h). The rescattering mechanism for the final-state-interaction (FSI) effects has been successfully applied to $D \rightarrow PV$ decays [50], B decays in $B \rightarrow \pi\pi, K\pi, D\pi$ [51] and KK channels [52]. In this work, we will again test the rescattering mechanism in $B^+ \rightarrow D_s^{*+} \bar{D}^0 \rightarrow D^+ X_0(2900)$ with K^0 exchange and $B^+ \rightarrow D_{s1}^+ \bar{D}^{*0} \rightarrow D^+ X_0(2900)$ with K^{*0} exchange, and other processes shown in Fig. 2. In order to reveal the nature of the observed $X_0(2900)$, we consider $X_0(2900)$ as $\bar{D}^* K^*$ molecule structure, scalar diquark-scalar antidiquark structure and axial vector diquark-axial vector antidiquark structure with QCD sum rule approach in this work.

This paper is organized as follows. In Sec. II, we derive the decay amplitudes for the diagrams in Fig. 2 via final state interaction. In Sec. III, we use the QCD sum rules method to study the three-point correlation functions for strong coupling for $X_0(2900)$ such as $\bar{D}^0 K^0 X_0$, $\bar{D}^{*0} K^{*0} X_0$ and other strong coupling such as $D_s^{*+} D^+ K^0$ and $D_{s1}^+ D^+ K^{*0}$ vertices. In Sec. IV, we will use the strong coupling constant obtained by QCD sum rules to calculate the amplitude and branching fraction for $B^+ \rightarrow D^+ X_0(2900)$ process. And finally we summarize our results in Sec. V.

II. FINAL STATE INTERACTION

In the framework of rescattering mechanism, the decay $B^+ \rightarrow D^+ X_0$ can most likely proceed as $B^+ \rightarrow D_s^{*+} \bar{D}^0 \rightarrow D^+ X_0(2900)$ with K^0 exchange and $B^+ \rightarrow D_{s1}^+ \bar{D}^{*0} \rightarrow D^+ X_0(2900)$ with K^{*0} exchange [24, 48], while other possible processes are also considered. Under the factorization approach [53, 54], we can get the decay amplitude of $B^+ \rightarrow D_s^{*+} \bar{D}^0$ and $B^+ \rightarrow D_{s1}^+ \bar{D}^{*0}$:

$$\begin{aligned}\mathcal{A}(B^+ \rightarrow D_s^{*+} \bar{D}^0) &= \frac{G_F}{\sqrt{2}} V_{cb} V_{cs} a_1 \langle D_s^{*+} | J_\mu^{(c\bar{s})} | 0 \rangle \langle \bar{D}^0 | J_\mu^W | B^+ \rangle, \\ \mathcal{A}(B^+ \rightarrow D_{s1}^+ \bar{D}^{*0}) &= \frac{G_F}{\sqrt{2}} V_{cb} V_{cs} a_1 \langle D_{s1}^+ | J_\mu^{(c\bar{s})} | 0 \rangle \langle \bar{D}^{*0} | J_\mu^W | B^+ \rangle,\end{aligned}\quad (4)$$

where G_F is the Fermi constant, V_{ik} is the CKM matrix elements, a_1 is the effective Wilson coefficients obtained by the factorization approach [55], and the effective operators $J_\mu^W, J_\mu^{(c\bar{s})}$ are defined as

$$\begin{aligned}J_\mu^W &= \bar{c} \gamma_\mu (1 - \gamma_5) b, \\ J_\mu^{(c\bar{s})} &= \bar{s} \gamma_\mu (1 - \gamma_5) c.\end{aligned}\quad (5)$$

The matrix elements in Eqs.(4) are defined as:

$$\begin{aligned}\langle 0 | J_\mu^{(c\bar{s})} | D_s^{*+}(p_1, \epsilon) \rangle &= \lambda_{D_s^{*+}} \epsilon_\mu, \\ \langle 0 | J_\mu^{(c\bar{s})} | D_{s1}^+(p_1, \epsilon) \rangle &= -\lambda_{D_{s1}^+} \epsilon_\mu, \\ \langle \bar{D}^0(p_2) | J_\mu^W | B^+(p) \rangle &= F_+(Q^2) P_\mu + F_-(Q^2) q_\mu, \\ \langle \bar{D}^{*0}(p_2, \epsilon) | J_\mu^W | B^+(p) \rangle &= \frac{i\epsilon^\nu}{m_B + m_{D^*}} \left\{ i\epsilon_{\mu\nu\alpha\beta} P^\alpha q^\beta A_V(Q^2) + (m_B + m_{D^*})^2 g_{\mu\nu} A_1(Q^2) - P_\mu P_\nu A_2(Q^2) \right. \\ &\quad \left. - 2m_{D^*}(m_B + m_{D^*}) \frac{P_\nu q_\mu}{q^2} (A_3(Q^2) - A_0(Q^2)) \right\},\end{aligned}\quad (6)$$

where $P_\mu = p_\mu + p_{2\mu}$, $q_\mu = p_\mu - p_{2\mu}$, $Q^2 = -q^2$ and $F_\pm(Q^2), A_{0,1,2,V}(Q^2)$ are the weak transition form factors. The form factors $F_\pm(Q^2)$ are related to the commonly used Bauer-Stech-Wirbel form factors via

$$F_+(Q^2) = F_1(Q^2), \quad (7)$$

$$F_-(Q^2) = \frac{m_B^2 - m_{D^*}^2}{Q^2} (F_1(Q^2) - F_0(Q^2)). \quad (8)$$

With the above hadronic matrix elements, the weak decay amplitude can be expressed as:

$$\mathcal{A}(B^+ \rightarrow D_s^{*+} \bar{D}^0) = i\sqrt{2} G_F V_{cb} V_{cs}^* a_1 \lambda_{D_s^{*+}} F_+^{B \rightarrow D} (-m_{D_s^{*+}}^2) \epsilon_{D_s^{*+}}^* \cdot p_{B^+} \quad (9)$$

$$\mathcal{A}(B^+ \rightarrow D_{s1}^+ \bar{D}^{*0}) = -\frac{G_F}{\sqrt{2}} \frac{V_{cb} V_{cs}^* a_1 \lambda_{D_{s1}^+}}{m_B + m_{D^*}} \left((m_B + m_{D^*})^2 (\epsilon_{D^*} \cdot \epsilon_{D_{s1}}) A_1(-m_{D_{s1}^+}^2) - 2(\epsilon_{D^*} \cdot p_B)(\epsilon_{D_{s1}} \cdot p_B) A_2(-m_{D_{s1}^+}^2) \right) \quad (10)$$

The amplitude for $B^+ \rightarrow D_s^{*+} \bar{D}^0 \rightarrow D^+ X_0(2900)$ process can be written as:

$$\begin{aligned} & \mathcal{A}(B^+ \rightarrow D_s^{*+} \bar{D}^0 \rightarrow D^+ X_0(2900)) \\ &= i\sqrt{2}G_F V_{cb} V_{cs}^* a_1 m_{X_0} \lambda_{D_s^*} F_+^{B \rightarrow D}(-m_{D_s^*}^2) \int_{-1}^1 \frac{|p_{D_s^*}| d\cos\theta d\phi}{32\pi^2 m_B} \frac{ig_{D_s^* DK}(-t)g_{DKX_0}(-t)}{t - m_K^2} H_1, \end{aligned} \quad (11)$$

where

$$H_1 = \left(\frac{(p_{D^0} \cdot p_{D_s^*})(p_{D^+} \cdot p_{D_s^*})}{m_{D_s^*}^2} - (p_{D^+} \cdot p_{D^0}) \right) (p_{D_s^*} \cdot p_{D^0} - p_{D^+} \cdot p_{D^0}). \quad (12)$$

The amplitude for $B^+ \rightarrow D_{s1} \bar{D}^* \rightarrow D^+ X_0(2900)$ process can be written as:

$$\begin{aligned} & \mathcal{A}(B^+ \rightarrow D_{s1} \bar{D}^* \rightarrow D^+ X_0(2900)) \\ &= -i \frac{G_F}{\sqrt{2}} V_{cb} V_{cs}^* a_1 \frac{i\lambda_{D_{s1}}}{(m_B + m_{D^*}^*)m_{D^*}^2 m_{D_{s1}}^2 m_{K^*}^2} \int_{-1}^1 \frac{|p_{D^*}| d\cos\theta d\phi}{32\pi^2 m_B} \frac{g_{D_{s1} DK^*}(-t)g_{D^* K^* X_0}(-t)}{t - m_{K^*}^2} (H_2 A_1(-m_{D_{s1}}^2) + 2H_3 A_2(-m_{D_{s1}}^2)), \end{aligned} \quad (13)$$

where

$$\begin{aligned} H_2 &= m_{D^*}^2 m_{D_{s1}}^2 (m_B + m_{D^*})^2 (m_D^2 - 2m_{K^*}^2) + m_{K^*}^2 (p_{D^*} \cdot p_{D_{s1}})^2 + m_{D^*}^2 (p_D \cdot p_{D_{s1}})^2 \\ &\quad + (p_{D^*} \cdot p_D - p_{D^*} \cdot p_{D_{s1}})(m_{D_{s1}}^2 p_{D^*} \cdot p_D - (p_{D^*} \cdot p_{D_{s1}}) \cdot (p_D \cdot p_{D_{s1}})), \\ H_3 &= m_{K^*}^2 p_{D^*} \cdot p_{D_{s1}} ((p_{D^*} \cdot p_{D_{s1}})^2 - m_{D^*}^2 m_{D_{s1}}^2) + (m_{D^*}^2 p_{D^*} \cdot p_D - (p_{D_{s1}} \cdot p_D)(p_{D^*} \cdot p_{D_{s1}})) \\ &\quad (m_{D^*}^2 (m_{D_{s1}}^2 - p_{D_{s1}} \cdot p_D) + p_{D^*} \cdot p_{D_{s1}} (p_{D^*} \cdot p_D - p_{D^*} \cdot p_{D_{s1}})). \end{aligned} \quad (14)$$

Similarly, the amplitude for the other processes shown in Fig. 2 can be written as:

$$\begin{aligned} \mathcal{A}(B^+ \rightarrow D_s \bar{D}^* \rightarrow D^+ X_0(2900)) &= -i \frac{G_F}{\sqrt{2}} V_{cb} V_{cs}^* a_1 \frac{i\lambda_{D_{s1}}}{m_D^2 m_{K^*}^2} ((m_B + m_{D^*})A_1(-m_{D_s}^2) - 2(m_B - m_{D^*})A_2(-m_{D_s}^2) \\ &\quad - 2m_{D^*}(A_3(-m_{D_s}^2) - A_0(-m_{D_s}^2))) \int_{-1}^1 \frac{|p_{D_s}| d\cos\theta d\phi}{32\pi^2 m_B} \frac{g_{D_s DK^*}(-t)g_{D^* K^* X_0}(-t)}{t - m_{K^*}^2} H_4, \end{aligned} \quad (15)$$

$$\begin{aligned} \mathcal{A}(B^+ \rightarrow D_{s0}^* \bar{D} \rightarrow D^+ X_0(2900)) &= i \frac{G_F}{\sqrt{2}} V_{cb} V_{cs}^* a_1 m_{X_0} \lambda_{D_s^*} (F_+^{B \rightarrow D}(-m_{D_{s0}^*}^2)(m_B^2 - m_D^2) + F_-^{B \rightarrow D}(-m_{D_{s0}^*}^2)) \\ &\quad \int_{-1}^1 \frac{|p_{D_{s0}^*}| d\cos\theta d\phi}{32\pi^2 m_B} \frac{ig_{D_{s0}^* DK}(-t)g_{DKX_0}(-t)}{t - m_K^2} (p_{D^+} \cdot p_{D_{s0}^*} - m_D^2)(p_{D_{s0}^*} \cdot p_{D^0} - p_{D^+} \cdot p_{D^0}), \end{aligned} \quad (16)$$

$$\begin{aligned} \mathcal{A}(B^+ \rightarrow D_s^* \bar{D}_1 \rightarrow D^+ X_0(2900)) &= i \frac{G_F}{\sqrt{2}} V_{cb} V_{cs}^* a_1 \frac{i\lambda_{D_s^*}}{(m_B + m_{D_1})m_{D_1}^2 m_{D_s^*}^2 m_{K_1}^2} \\ &\quad \int_{-1}^1 \frac{|p_{D_1}| d\cos\theta d\phi}{32\pi^2 m_B} \frac{g_{D_s^* DK_1}(-t)g_{D_1 K_1 X_0}(-t)}{t - m_{K_1}^2} (H_5 A_1(-m_{D_s^*}^2) + 2H_6 A_2(-m_{D_s^*}^2)), \end{aligned} \quad (17)$$

$$\begin{aligned} \mathcal{A}(B^+ \rightarrow D_{s0}^* \bar{D}_1 \rightarrow D^+ X_0(2900)) &= i \frac{G_F}{\sqrt{2}} V_{cb} V_{cs}^* a_1 \frac{i\lambda_{D_s^*}}{m_{D_1}^2 m_{K_1}^2} ((m_B + m_{D_1})A_1(-m_{D_{s0}^*}^2) - 2(m_B - m_{D_1})A_2(-m_{D_{s0}^*}^2) \\ &\quad - 2m_{D_1}(A_3(-m_{D_{s0}^*}^2) - A_0(-m_{D_{s0}^*}^2))) \int_{-1}^1 \frac{|p_{D_{s0}^*}| d\cos\theta d\phi}{32\pi^2 m_B} \frac{g_{D_{s0}^* DK_1}(-t)g_{D_1 K_1 X_0}(-t)}{t - m_{K_1}^2} H_7, \end{aligned} \quad (18)$$

$$\begin{aligned} \mathcal{A}(B^+ \rightarrow D_s \bar{D}_0^* \rightarrow D^+ X_0(2900)) &= -i \frac{G_F}{\sqrt{2}} V_{cb} V_{cs}^* a_1 m_{X_0} \lambda_{D_{s1}} (F_+^{B \rightarrow D_0^*}(-m_{D_s}^2)(m_B^2 - m_D^2) + F_-^{B \rightarrow D_0^*}(-m_{D_s}^2)) \\ &\quad \int_{-1}^1 \frac{|p_{D_s}| d\cos\theta d\phi}{32\pi^2 m_B} \frac{ig_{D_s DK_0^*}(-t)g_{D_0^* K_0^* X_0}(-t)}{t - m_{K_0^*}^2} (p_{D^+} \cdot p_{D_s})(p_{D_s} \cdot p_{D^*} - p_{D^+} \cdot p_{D^*}), \end{aligned} \quad (19)$$

$$\mathcal{A}(B^+ \rightarrow D_{s1} \bar{D}_0^* \rightarrow D^+ X_0(2900)) = -i\sqrt{2}G_F V_{cb} V_{cs}^* a_1 m_{X_0} \lambda_{D_{s1}} F_+^{B \rightarrow D}(-m_{D_s^*}^2) \int_{-1}^1 \frac{|p_{D_s^*}| d\cos\theta d\phi}{32\pi^2 m_B} \frac{ig_{D_s^* DK}(-t)g_{DKX_0}(-t)}{t - m_K^2} H_8, \quad (20)$$

where

$$H_4 = (m_D^2 - m_{D^*}^2 + m_{K^*}^2)(m_{D_s}^2 m_{D^*}^2 - (p_{D_s} \cdot p_{D^0})^2)$$

$$+(m_D^2 - m_{D^*}^2 - m_{K^*}^2)((p_{D_s} \cdot p_{\bar{D}^{*0}})(p_{D^+} \cdot p_{\bar{D}^{*0}}) - m_{D^*}^2(p_{D_s} \cdot p_{D^+})), \quad (21)$$

$$H_5 = m_{D_1}^2 m_{D_s^*}^2 (m_B + m_{D_1})^2 (m_D^2 - 2m_{K_1}^2) + m_{K_1}^2 (p_{D_1} \cdot p_{D_s^*})^2 + m_{D_1}^2 (p_D \cdot p_{D_s^*})^2 \\ + (p_{D_1} \cdot p_D - p_{D_1} \cdot p_{D_s^*}) (m_{D_s^*}^2 p_{D_1} \cdot p_D - (p_{D_1} \cdot p_{D_s^*}) \cdot (p_D \cdot p_{D_s^*})), \quad (22)$$

$$H_6 = m_{K_1}^2 p_{D_1} \cdot p_{D_s^*} ((p_{D_1} \cdot p_{D_s^*})^2 - m_{D_1}^2 m_{D_s^*}^2) + (m_{D_1}^2 p_{D_1} \cdot p_D - (p_{D_s^*} \cdot p_D)(p_{D_1} \cdot p_{D_s^*})) \\ (m_{D_1}^2 (m_{D_s^*}^2 - p_{D_s^*} \cdot p_D) + p_{D_1} \cdot p_{D_s^*} (p_{D_1} \cdot p_D - p_{D_1} \cdot p_{D_s^*})), \quad (23)$$

$$H_7 = m_D^2 (m_{D_{s0}}^2 m_{D_1}^2 - (p_{D_{s0}} \cdot p_{D_1})^2) + (p_{D_{s0}} \cdot p_{D_1})(p_{D^+} \cdot p_{D_1})(m_D^2 - m_{K_1}^2 - p_{D_{s0}} \cdot p_{D^+}) \\ + (p_{D_{s0}} \cdot p_{D^+})(m_{D_1}^2 (p_{D_{s0}} \cdot p_{D^+} - m_D^2 - m_{D_{s0}}^2 + m_{K_1}^2) + (p_{D_{s0}} \cdot p_{D_1})^2), \quad (24)$$

$$H_8 = \left(\frac{(p_{D^*} \cdot p_{D_{s1}})(p_{D^+} \cdot p_{D_{s1}})}{m_{D_{s1}}^2} - (p_{D^+} \cdot p_{D^*}) \right) (p_{D_{s1}} \cdot p_{D^*} - p_{D^+} \cdot p_{D^*}). \quad (25)$$

It should be noted that in Ref.[48], the decay amplitude in Eq. (11) contains the form factor $F(t, m) = (\Lambda^2 - m_K^2)/(\Lambda^2 - t)$ for each strong vertices, which is introduced to compensate the off-shell effect of the exchanged particle at the vertices [56]. In Ref. [57], the authors claim that the monopole behavior of the form factor is preferred as it is consistent with the QCD sum rule expectation. The cutoff Λ is usually chosen as

$$\Lambda = m_K + \eta \Lambda_{\text{QCD}}, \quad (26)$$

and the amplitude would be very sensitive to the value of η . However, we will see with QCD sum rule approach in the next section, the form factor does not always behave as a monopole model. With the above consideration, we shall replace the g_{ABC} with $F(t, m)$ given in the Ref. [48] by $g_{ABC}(Q^2)$ for a ABC strong vertex shown in Eq. (11) and (13). In the next section, we shall obtain the coupling constant in Eq. (11) and (13) with QCD sum rule approach and show that the coupling constant $g_{ABC}(Q^2)$ does not always behave as a monopole model.

III. THREE-POINT QCD SUM RULE

Over past several decades, the method of QCD sum rules has been proven to be very powerful to study hadron properties [58–61]. In this section, we shall study the three-point correlation function of several two-body strong decay process $M \rightarrow X + Y$. For the strong decay process $M \rightarrow X + Y$, the corresponding correlator is written as

$$\Pi(p, p', q) = \int d^4x d^4y e^{ip' \cdot x} e^{iq \cdot y} \langle 0 | T \{ J_X(x) J_Y(y) J_M^\dagger(0) \} | 0 \rangle, \quad (27)$$

where $J_{M(X,Y)}$ is the interpolating current for the initial(final) state. In this section, we shall consider the $\bar{D}KX_0$, $\bar{D}^*K^*X_0$, $\bar{D}_1K_1X_0$, $\bar{D}_0^*K_0^*X_0$ strong decay vertices with $K(K^*, K_1, K_0^*)$ off shell and D_s^*DK , $D_{s1}DK^*$, $D_{s0}DK$, D_sDK^* , $D_s^*DK_1$, $D_{s0}DK_1^*$, $D_s^*DK_0^*$, $D_{s1}DK_0^*$ strong decay vertices with $K(K^*, K_1, K_0^*)$ off shell. Some of these strong decay vertices are studied by some previous QCD sum rule analysis. We use the following interpolating currents for $X_0(2900)$ by considering it as a \bar{D}^*K^* molecule, scalar diquark-scalar antidiquark compact tetraquark and axial-vector diquark-axial-vector antidiquark compact tetraquark:

$$J_{X_0(\text{mol})} = \bar{c}_a \gamma_\mu d_a \bar{s}_b \gamma_\mu u_b, \quad (28)$$

$$J_{X_0(\text{S-S})} = \epsilon_{abc} \epsilon_{efc} (u_a^T C \gamma_5 d_b) (\bar{c}_e \gamma_5 C \bar{s}_f^T), \quad (29)$$

$$J_{X_0(\text{A-A})} = \epsilon_{abc} \epsilon_{efc} (u_a^T C \gamma_\mu d_b) (\bar{c}_e \gamma_\mu C \bar{s}_f^T), \quad (30)$$

where $a \cdots f$ denote the color index and u, d, s, c denote the up, down, strange, charm quark field, respectively. These current can couple to the $X_0(2900)$ state via

$$\langle 0 | J_{X_0(\text{mol})} | X_0(2900) \rangle = \lambda_{X_0(\text{mol})}, \quad (31)$$

$$\langle 0 | J_{X_0(\text{S-S})} | X_0(2900) \rangle = \lambda_{X_0(\text{S-S})}, \quad (32)$$

$$\langle 0 | J_{X_0(\text{A-A})} | X_0(2900) \rangle = \lambda_{X_0(\text{A-A})}, \quad (33)$$

in which the value of the coupling constant λ_{X_0} are determined from the two-point mass sum rules established in Ref. [29, 30, 39] :

$$\lambda_{X_0(\text{mol})}/m_{X_0} = (3.0 \pm 0.7) \times 10^{-3} \text{GeV}^5, \\ \lambda_{X_0(\text{S-S})}/m_{X_0} = (1.2 \pm 0.2) \times 10^{-2} \text{GeV}^5, \\ \lambda_{X_0(\text{A-A})}/m_{X_0} = (1.6 \pm 0.3) \times 10^{-2} \text{GeV}^5. \quad (34)$$

The other hadronic parameters in this work are listed in Tab. I.

TABLE I: The values of the hadronic parameters m_H and f_H in the work taken from Ref. [3, 62, 63].

Hadron(H)	Mass m_H [GeV]	Decay constant f_H [GeV]	Hadron(H)	Mass m_H [GeV]	Decay constant f_H [GeV]
D	1.87	0.20 ± 0.02	D^*	2.01	0.24 ± 0.04
D_s	1.97	0.24 ± 0.04	D_s^*	2.11	0.29 ± 0.05
K	0.49	0.16 ± 0.02	K^*	0.89	0.22 ± 0.01
D_1	2.42	0.27 ± 0.01	D_0^*	2.34	0.10 ± 0.01
D_{s1}	2.46	0.23 ± 0.02	D_{s0}^*	2.32	0.18 ± 0.03
K_1	1.25	0.25 ± 0.01	K_0^*	0.85	0.19 ± 0.01

A. Coupling constant of $X_0(2900)$

In this subsection, we study the strong vertex $\bar{D}KX_0$ and $\bar{D}^*K^*X_0$ with \bar{D}^*K^* molecule interpretation for $X_0(2900)$ state as an example. The interpolating currents for $\bar{D}^{(*)}$ and K^{*0} mesons are

$$\begin{aligned}
J_{\bar{D}} &= i\bar{c}_a\gamma_5 u_a, \\
J_{\bar{D}^*\mu} &= \bar{c}_a\gamma_\mu u_a, \\
J_{K^0} &= i\bar{s}_a\gamma_5 d_a, \\
J_{K^{*0}\mu} &= \bar{s}_a\gamma_\mu d_a.
\end{aligned} \tag{35}$$

They can couple to the corresponding mesons via the following relations

$$\begin{aligned}
\langle 0|J_{\bar{D}}|\bar{D}\rangle &= f_{\bar{D}}\frac{m_{\bar{D}}^2}{m_c} \equiv \lambda_{\bar{D}}, \\
\langle 0|J_{K^0}|K^0\rangle &= f_K\frac{m_K^2}{m_s} \equiv \lambda_K, \\
\langle 0|J_{\bar{D}^*\mu}|\bar{D}^*\rangle &= m_{\bar{D}^*}f_{\bar{D}^*}\epsilon_\mu \equiv \lambda_{\bar{D}^*}\epsilon_\mu, \\
\langle 0|J_{K^{*0}\mu}|K^{*0}\rangle &= m_{K^*}f_{K^*}\epsilon_\mu \equiv \lambda_{K^*}\epsilon_\mu.
\end{aligned} \tag{36}$$

Here $f_{\bar{D}}$, f_K , $f_{\bar{D}^*}$, f_{K^*} are the decay constants of the \bar{D} , K , \bar{D}^* , K^* mesons. ϵ_μ is the polarization vector. The coupling constant $g_{\bar{D}KX_0}$ and $g_{\bar{D}^*K^*X_0}$ are defined via the effective Lagrangian [45, 64]

$$\mathcal{L}_{\bar{D}KX_0} = g_{\bar{D}KX_0}m_{X_0}X_0\partial^\mu\bar{D}\partial_\mu K, \tag{37}$$

$$\mathcal{L}_{\bar{D}^*K^*X_0} = g_{\bar{D}^*K^*X_0}X_0\bar{D}^{*\mu}K_\mu^*, \tag{38}$$

thus the transition matrix element can be obtained as

$$\langle \bar{D}(p)K^0(q)|X_0(p')\rangle = g_{\bar{D}KX_0}m_{X_0}p \cdot q, \tag{39}$$

$$\langle \bar{D}^*(p)K^{*0}(q)|X_0(p')\rangle = g_{\bar{D}^*K^*X_0}\epsilon(p) \cdot \epsilon(q). \tag{40}$$

With the above coupling relations and transition matrix element, we can obtain the three-point correlation function Eq.(27) for $\bar{D}K \rightarrow X_0$ process on the phenomenological side

$$\begin{aligned}
\Pi(p, p', q) &= \int d^4x d^4y e^{ip' \cdot x} e^{-iq \cdot y} \langle 0|T\{J_{X_0}(x)J_{K^0}^\dagger(y)J_{\bar{D}}^\dagger(0)\}|0\rangle \\
&= \frac{\lambda_{X_0}\lambda_{\bar{D}}\lambda_K g_{\bar{D}KX_0}m_{X_0}(p \cdot q)}{(p'^2 - m_{X_0}^2)(p^2 - m_{\bar{D}}^2)(q^2 - m_K^2)} + \dots
\end{aligned} \tag{41}$$

On the OPE side, we can evaluate the correlation function with standard QCD sum rules approach. To establish a sum rule for the coupling constant, we will pick out the $1/q^2$ terms around the pole $q^2 \sim 0$ with the structure $p \cdot q$ in the OPE series and then match

both sides of the sum rule. To apply sum rules appropriately, we shall calculate at Q^2 far away from the on-shell mass $-m_K^2$ to ensure the approximation $p^2 = p'^2 = P^2$ valid. After performing the Borel transform $P^2 \rightarrow M_B^2$ on both phenomenological and OPE sides, we obtain

$$g_{\bar{D}KX_0}(s_0, M_B^2) = \frac{1}{\lambda_{X_0} \lambda_{\bar{D}} \lambda_K m_{X_0}} \frac{m_{X_0}^2 - m_D^2}{e^{-m_D^2/M_B^2} - e^{-m_{X_0}^2/M_B^2}} \left(\frac{Q^2 + m_K^2}{Q^2} \right) \left(\int_{s_0}^{s_c} ds \rho(s) e^{-s/M_B^2} + R(M_B^2) e^{-m_c^2/M_B^2} \right), \quad (42)$$

where the continuum threshold $s_0 = 10 \text{ GeV}^2$ is taken from the two-point mass sum rules in Ref. [38]. The spectrum function $\rho(s)$ and $R(M_B^2)$ are given in Appendix A, and the Feynman diagram we considered are shown in Fig. 3.

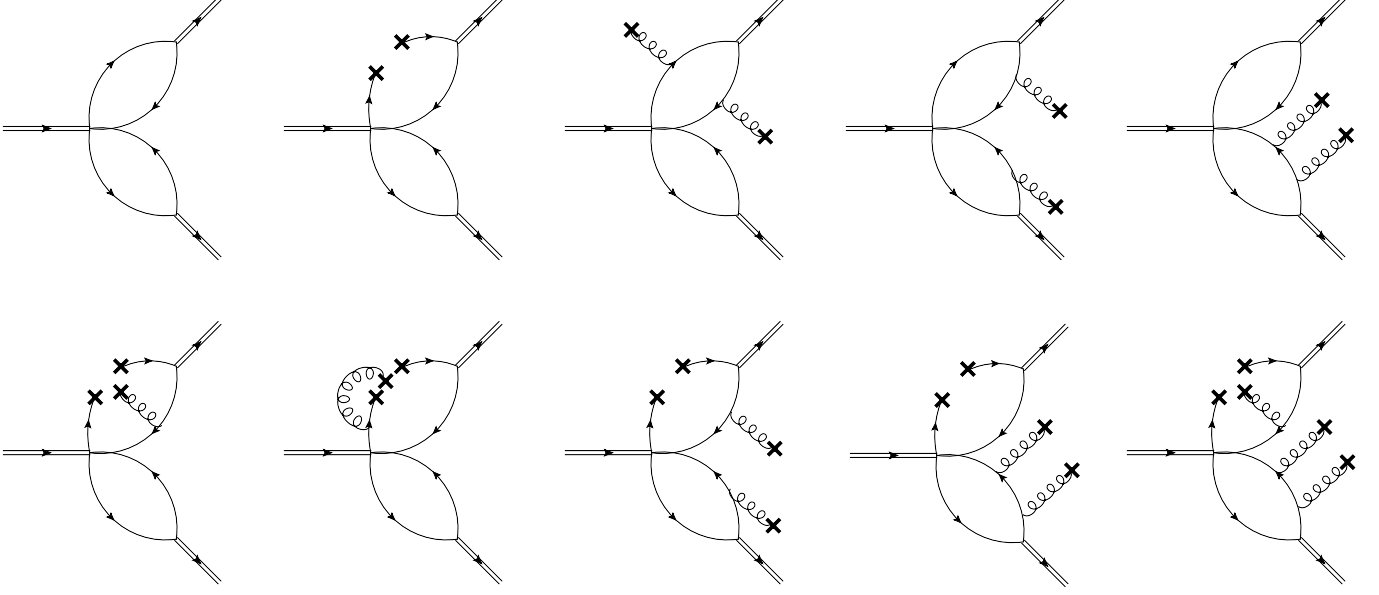


FIG. 3: The Feynman diagrams for OPE series of the correlation function in (42). The double solid line denotes the in(out)-coming hadron, while the single solid line denotes the quark propagator. Diagrams related by symmetry are not shown.

We use the standard values of various QCD condensates as $\langle \bar{q}q \rangle(1\text{GeV}) = -(0.24 \pm 0.03)^3 \text{ GeV}^3$, $\langle \bar{q}g_s\sigma \cdot Gq \rangle(1\text{GeV}) = -M_0^2 \langle \bar{q}q \rangle$, $M_0^2 = (0.8 \pm 0.2) \text{ GeV}^2$, $\langle \bar{s}s \rangle / \langle \bar{q}q \rangle = 0.8 \pm 0.1$, $\langle g_s^2 GG \rangle(1\text{GeV}) = (0.48 \pm 0.14) \text{ GeV}^4$ at the energy scale $\mu = 1\text{GeV}$ [65–72] and $m_s(2 \text{ GeV}) = 95^{+9}_{-3} \text{ MeV}$, $m_c(m_c) = 1.27^{+0.03}_{-0.04} \text{ GeV}$, $m_b(m_b) = 4.18^{+0.04}_{-0.03} \text{ GeV}$ from the Particle Data Group[3]. These values are widely used in the previous QCD sum rules for traditional baryon states, meson states, multiquark states, etc., and provide experimentally consistent results [5, 10, 58, 65]. We also take into account the energy-scale dependence of the above parameters from the renormalization group equation

$$\begin{aligned} m_s(\mu) &= m_s(2\text{GeV}) \left[\frac{\alpha_s(\mu)}{\alpha_s(2\text{GeV})} \right]^{\frac{12}{33-2n_f}}, \\ m_c(\mu) &= m_c(m_c) \left[\frac{\alpha_s(\mu)}{\alpha_s(m_c)} \right]^{\frac{12}{33-2n_f}}, \\ m_b(m_b) &= m_b(m_b) \left[\frac{\alpha_s(\mu)}{\alpha_s(m_b)} \right]^{\frac{12}{33-2n_f}}, \\ \langle \bar{q}q \rangle(\mu) &= \langle \bar{q}q \rangle(1\text{GeV}) \left[\frac{\alpha_s(1\text{GeV})}{\alpha_s(\mu)} \right]^{\frac{12}{33-2n_f}}, \\ \langle \bar{s}s \rangle(\mu) &= \langle \bar{s}s \rangle(1\text{GeV}) \left[\frac{\alpha_s(1\text{GeV})}{\alpha_s(\mu)} \right]^{\frac{12}{33-2n_f}}, \\ \langle \bar{q}g_s\sigma \cdot Gq \rangle(\mu) &= \langle \bar{q}g_s\sigma \cdot Gq \rangle(1\text{GeV}) \left[\frac{\alpha_s(1\text{GeV})}{\alpha_s(\mu)} \right]^{\frac{2}{33-2n_f}}, \\ \langle \bar{s}g_s\sigma \cdot Gs \rangle(\mu) &= \langle \bar{s}g_s\sigma \cdot Gs \rangle(1\text{GeV}) \left[\frac{\alpha_s(1\text{GeV})}{\alpha_s(\mu)} \right]^{\frac{2}{33-2n_f}}, \end{aligned} \quad (43)$$

$$\alpha_s(\mu) = \frac{1}{b_0 t} \left[1 - \frac{b_1}{b_0} \frac{\log t}{t} + \frac{b_1^2 (\log^2 t - \log t - 1) + b_0 b_2}{b_0^4 t^2} \right],$$

where $t = \log \frac{\mu^2}{\Lambda^2}$, $b_0 = \frac{33-2n_f}{12\pi}$, $b_1 = \frac{153-19n_f}{24\pi^2}$, $b_2 = \frac{2857 - \frac{5033}{9}n_f + \frac{325}{27}n_f^2}{128\pi^3}$, $\Lambda = 210$ MeV, 292 MeV and 332 MeV for the flavors $n_f = 5, 4$ and 3, respectively. In this work, we evolve all the input parameters to the energy scale $\mu = m_c$ for our sum rule analysis. The parameters for the $D^{(*)}$ and $K^{(*)}$ mesons are adopted in Tab. I.

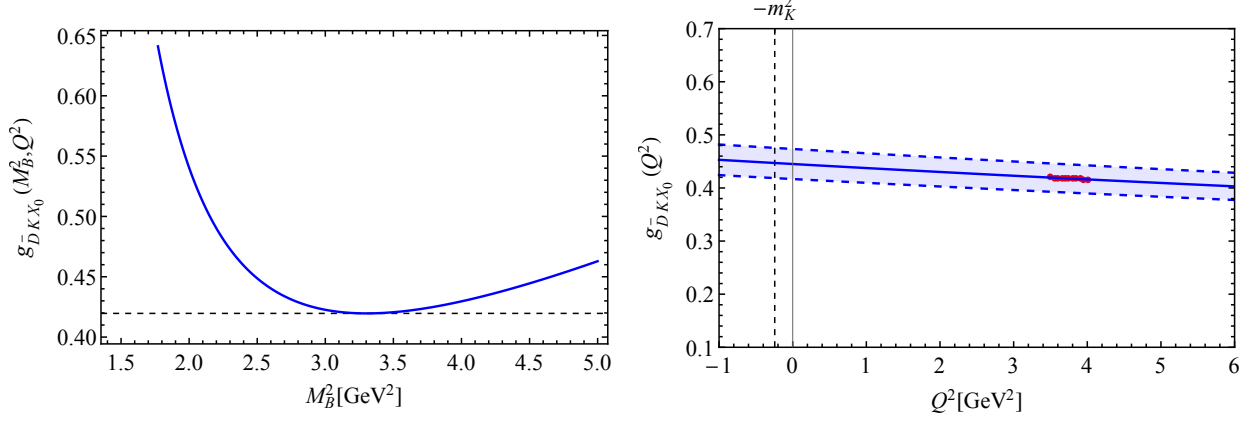


FIG. 4: The dependence of the coupling constant $g_{\bar{D}^{*}KX_0}$ on the Borel mass M_B^2 (left panel) and transfer momentum Q^2 (right panel). On the left panel, the transfer momentum is set to be $Q^2 = m_D^2 \sim 3.5$ GeV². On the right panel, the red dots denote the value from Eq.(42) with $s_0 = 10$ GeV² and $M_B^2 = 3.30$ GeV². The blue solid line is the monopolar fitting curve. The two dashed blue lines denote the upper and lower boundary of the uncertainty from various condensates, quark masses and hadronic parameters.

In the left panel of Fig.4, we show the variation of the coupling constant $g_{\bar{D}^{*}KX_0}(Q^2)$ with the Borel mass M_B^2 at $Q^2 = m_D^2 \sim 3.5$ GeV². Such a momentum point is chosen far away from m_K^2 so that it can be safely ignored and the OPE series is valid in this region. We find that the coupling constant $g_{\bar{D}^{*}KX_0}(Q^2)$ has a minimum value at $M_B^2 \sim 3.30$ GeV², around which it has minimal dependence on the non-physical parameter M_B^2 . To extrapolate the coupling constant from the valid QCD sum rule working region to the physical pole $Q^2 = -m_K^2$, we fit the sum rule result for $s_0 = 10$ GeV² and $M_B^2 = 3.30$ GeV² with monopolar model

$$g_{\bar{D}^{*}KX_0}(Q^2) = \frac{a}{b + Q^2}. \quad (44)$$

The fitting curve is shown in the right panel of Fig.4, and the result is as follow:

$$g_{\bar{D}^{*}KX_0}(Q^2) = \frac{(25.56 \pm 1.63) \text{ GeV}^2}{Q^2 + (57.43 \pm 0.00) \text{ GeV}^2}. \quad (45)$$

As for $\bar{D}^{*}K^{*} \rightarrow X_0$ process

$$\begin{aligned} \Pi(p, p', q) &= \int d^4x d^4y e^{ip' \cdot x} e^{-iq \cdot y} \langle 0 | T \{ J_{X_0}(x) J_{K^{*}0\mu}^{\dagger}(y) J_{\bar{D}^{*}\mu}^{\dagger}(0) | 0 \rangle \\ &= \frac{\lambda_{X_0} \lambda_{\bar{D}^{*}} \lambda_{K^{*}} g_{\bar{D}^{*}K^{*}X_0}}{(p'^2 - m_{X_0}^2)(p^2 - m_{D^{*}}^2)(q^2 - m_{K^{*}}^2)} \left(3 + \frac{Q^2}{m_{K^{*}}^2} + \frac{(Q^2 - m_{D^{*}}^2 + m_{X_0}^2)^2}{4m_{D^{*}}^2 m_{K^{*}}^2} \right) + \dots \end{aligned} \quad (46)$$

After performing the Borel transform $P^2 \rightarrow M_B^2$ on both phenomenological and OPE sides, we obtain

$$\begin{aligned} g_{\bar{D}^{*}K^{*}X_0}(s_0, M_B^2) &= \frac{1}{\lambda_{X_0} \lambda_{\bar{D}^{*}} \lambda_{K^{*}} m_{X_0}} \frac{m_{X_0}^2 - m_D^{*2}}{e^{-m_D^{*2}/M_B^2} - e^{-m_{X_0}^2/M_B^2}} \frac{Q^2 + m_K^{*2}}{Q^2} \\ &\quad \left(\frac{4m_{D^{*}}^2 m_{K^{*}}^2}{12m_{D^{*}}^2 m_{K^{*}}^2 + ((m_{X_0} - m_{D^{*}})^2 + Q^2)((m_{X_0} + m_{D^{*}})^2 + Q^2)} \right) \left(\int_{s_c}^{s_0} ds \rho(s) e^{-s/M_B^2} + R(M_B^2) e^{-m_c^2/M_B^2} \right), \end{aligned} \quad (47)$$

where the spectral function $\rho(s)$ and $R(M_B^2)$ are given in Appendix A.

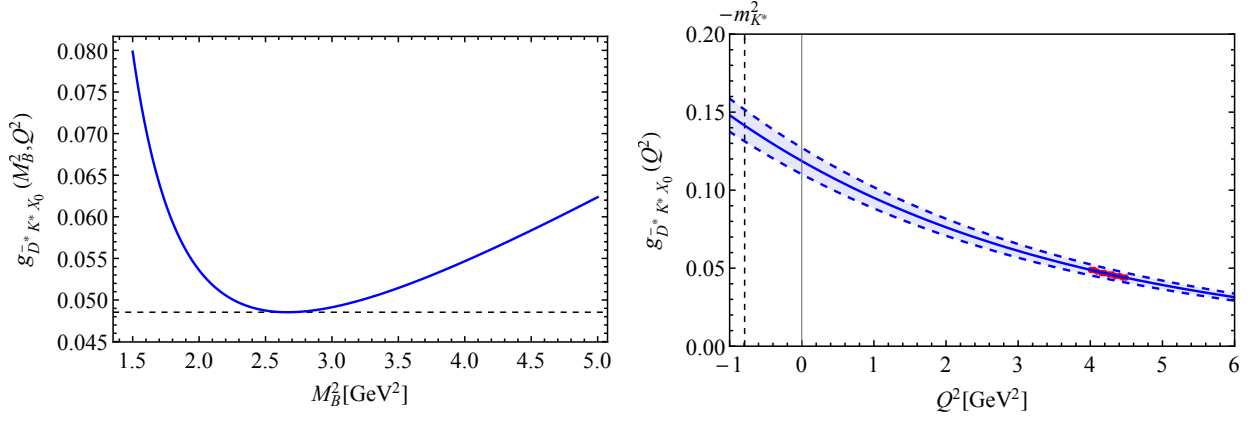


FIG. 5: The dependence of the coupling constant $g_{\bar{D}^* K^* X_0}$ on the Borel mass M_B^2 (left panel) and transfer momentum Q^2 (right panel). On the left panel, the transfer momentum is set to be $Q^2 = m_{D^*}^2 \sim 4 \text{ GeV}^2$. On the right panel, the red dots denote the value from Eq.(42) with $s_0 = 10 \text{ GeV}^2$ and $M_B^2 = 2.56 \text{ GeV}^2$. The blue solid line is the exponential fitting curve. The two dashed blue lines denote the upper and lower boundary of the uncertainty from various condensates, quark masses and hadronic parameters.

In the left panel of Fig.5, we show the variation of the coupling constant $g_{\bar{D}^* K^* X_0}(Q^2)$ with the Borel mass M_B^2 at $Q^2 = m_{D^*}^2 \sim 4 \text{ GeV}^2$. Such a momentum point is chosen far away from $m_{K^*}^2$ so that it can be safely ignored and the OPE series is valid in this region. We find that the coupling constant $g_{\bar{D}^* K^* X_0}(Q^2)$ has a minimum value at $M_B^2 \sim 2.56 \text{ GeV}^2$, around which it has minimal dependence on the non-physical parameter M_B^2 . We find that the results can be well fitted by the exponential model

$$g_{\bar{D}^* K^* X_0}(Q^2) = a e^{-b Q^2}. \quad (48)$$

The fitting curve is shown in the right panel of Fig.5, and the result is as follow:

$$g_{\bar{D}^* K^* X_0}(Q^2) = (0.12^{+0.008}_{-0.008} \text{ GeV}^2) e^{-(0.22 \pm 0.00) \text{ GeV}^{-2} Q^2}. \quad (49)$$

Similarly, we can obtain the coupling constant $g_{D_1 K_1 X_0}$ and $g_{D_0 K_0 X_0}$ with interpolating currents

$$\begin{aligned} J_{D_0^*} &= \bar{c}_a u_a, \\ J_{\bar{D}_{1\mu}} &= \bar{c}_a \gamma_\mu \gamma_5 u_a, \\ J_{K_0^0} &= \bar{s}_a d_a, \\ J_{K_{1\mu}} &= \bar{s}_a \gamma_\mu \gamma_5 d_a. \end{aligned} \quad (50)$$

with the following coupling relations

$$\begin{aligned} \langle 0 | J_{\bar{D}_0^*} | \bar{D}_0^* \rangle &= \lambda_{\bar{D}_0^*}, \\ \langle 0 | J_{K_0^*} | K_0^* \rangle &= \lambda_{K_0^*}, \\ \langle 0 | J_{\bar{D}_{1\mu}} | \bar{D}_1^* \rangle &= \lambda_{\bar{D}_1} \epsilon_\mu, \\ \langle 0 | J_{K_{1\mu}} | K_1^0 \rangle &= \lambda_{K_1} \epsilon_\mu. \end{aligned} \quad (51)$$

and the transition matrix

$$\langle \bar{D}_1(p) K_1^0(q) | X_0(p') \rangle = g_{\bar{D}_1 K_1 X_0} \epsilon(p) \cdot \epsilon(q), \quad (52)$$

$$\langle \bar{D}_0^*(p) K_0^{*0}(q) | X_0(p') \rangle = g_{\bar{D}_0^* K_0^* X_0} m_{X_0} p \cdot q. \quad (53)$$

The sum rule for coupling constant $g_{\bar{D}_1 K_1 X_0}$ and $g_{\bar{D}_0^* K_0^* X_0}$ can be obtained as follow:

$$\begin{aligned} g_{\bar{D}_1 K_1 X_0}(s_0, M_B^2) &= \frac{1}{\lambda_{X_0} \lambda_{\bar{D}_1} \lambda_{K_1} m_{X_0}} \frac{m_{X_0}^2 - m_{D_1}^2}{e^{-m_{D_1}^2/M_B^2} - e^{-m_{X_0}^2/M_B^2}} \frac{Q^2 + m_{K_1}^2}{Q^2} \\ &\quad \left(\frac{4m_{D_1}^2 m_{K_1}^2}{12m_{D_1}^2 m_{K_1}^2 + ((m_{X_0} - m_{D_1})^2 + Q^2)((m_{X_0} + m_{D_1})^2 + Q^2)} \right) \left(\int_{s_c}^{s_0} ds \rho(s) e^{-s/M_B^2} + R(M_B^2) e^{-m_c^2/M_B^2} \right), \end{aligned} \quad (54)$$

$$g_{\bar{D}_0 K_0 X_0}(s_0, M_B^2) = \frac{1}{\lambda_{X_0} \lambda_{\bar{D}_0^*} \lambda_{K_0^*} m_{X_0}} \frac{m_{X_0}^2 - m_{D_0^*}^2}{e^{-m_{D_0^*}^2/M_B^2} - e^{-m_{X_0}^2/M_B^2}} \left(\frac{Q^2 + m_{K_0^*}^2}{Q^2} \right) \left(\int_{s_0}^{\infty} ds \rho(s) e^{-s/M_B^2} + R(M_B^2) e^{-m_c^2/M_B^2} \right), \quad (55)$$

The results for coupling constant $g_{\bar{D}_1 K_1 X_0}$ and $g_{\bar{D}_0 K_0 X_0}$ are similar as above, as well as other two interpretation of $X_0(2900)$, thus we only list out the results in Tab. II and leave out the redundant discussion. The continuum thresholds s_0 for the compact structures are taken from Ref. [32].

TABLE II: Fitting coefficients with different models of coupling constant $g_{\bar{D}_{(0,1)}^{(*)} K_{(0,1)}^{(*)} X_0}$ for different $X_0(2900)$'s structures

Coupling constant	Structure of $X_0(2900)$	Model			
		$a/(b + Q^2)$		$a \text{Exp}(-b Q^2)$	
		$a[\text{GeV}^2]$	$b[\text{GeV}^2]$	$a[\text{GeV}^2]$	$b[\text{GeV}^{-2}]$
$g_{\bar{D} K X_0}$	$\bar{D}^* K^*$ Molecule	25.56 ± 1.63	57.43 ± 0.00	-	-
	S – S Tetraquark	18.20 ± 1.97	57.43 ± 0.00	-	-
	A – A Tetraquark	22.20 ± 3.94	57.43 ± 0.00	-	-
$g_{\bar{D}^* K^* X_0}$	$\bar{D}^* K^*$ Molecule	-	-	$0.12^{+0.008}_{-0.008}$	0.22 ± 0.00
	S – S Tetraquark	-	-	$0.04^{+0.015}_{-0.007}$	0.22 ± 0.00
	A – A Tetraquark	-	-	$0.04^{+0.031}_{-0.014}$	0.22 ± 0.00
$g_{\bar{D}_1 K_1 X_0}$	$\bar{D}^* K^*$ Molecule	-	-	0.38 ± 0.01	$0.03^{+0.05}_{-0.02}$
	S – S Tetraquark	-	-	0.10 ± 0.03	0.03 ± 0.01
	A – A Tetraquark	-	-	0.20 ± 0.02	0.03 ± 0.01
$g_{\bar{D}_0^* K_0^* X_0}$	$\bar{D}^* K^*$ Molecule	$13.59^{+5.07}_{-6.21}$	46.23 ± 0.00	-	-
	S – S Tetraquark	$2.11^{+0.44}_{-0.63}$	51.19 ± 0.07	-	-
	A – A Tetraquark	$3.86^{+0.92}_{-0.90}$	46.23 ± 0.01	-	-

B. Coupling constant $g_{\bar{D}_{s(0,1)}^{(*)} D K_{s(0,1)}^{(*)}}$

In this subsection, we consider the other strong coupling vertex in Fig. 2. The interpolating currents for the relevant mesons are

$$\begin{aligned} J_{D_s} &= i\bar{s}\gamma_5 c, & J_{D_{s0}^*} &= \bar{s}c, \\ J_{D_s^*} &= \bar{s}\gamma_\mu c, & J_{D_{s1}} &= \bar{s}\gamma_\mu \gamma_5 c, \\ J_{D^{*+}} &= i\bar{d}\gamma_5 c. \end{aligned} \quad (56)$$

They can couple to the corresponding mesons via the following relations

$$\begin{aligned} \langle 0 | J_{D_s} | D_s \rangle &= f_{D_s} \frac{m_{D_s}^2}{m_c} \equiv \lambda_{D_s}, & \langle 0 | J_{D_{s0}^*} | D_{s0}^* \rangle &= f_{D_{s0}^*} \frac{m_{D_{s0}^*}^2}{m_c} \equiv \lambda_{D_{s0}^*}, \\ \langle 0 | J_{D_{s\mu}^*} | D_s^*(p, \epsilon) \rangle &= m_{D_s^*} f_{D_s^*} \epsilon_\mu \equiv \lambda_{D_s^*} \epsilon_\mu, & \langle 0 | J_{D_{s1}} | D_{s1}(p', \epsilon) \rangle &= m_{D_{s1}} f_{D_{s1}} \epsilon_\mu \equiv \lambda_{D_{s1}} \epsilon_\mu, \\ \langle 0 | J_{D^{*+}} | D^+ \rangle &= f_D \frac{m_D^2}{m_c} \equiv \lambda_D. \end{aligned} \quad (57)$$

The coupling constant $g_{\bar{D}_{s(0,1)}^{(*)} D_{s(0,1)}^{(*)} K_{s(0,1)}^{(*)}}$ in Eqs.(13)-(20) are defined via the effective Lagrangian [73–75]

$$\begin{aligned} \mathcal{L}_{\bar{D}_s^* D K} &= -i g_{\bar{D}_s^* D K} \left(D \partial^\mu K D_{s\mu}^{*\dagger} - D_{s\mu}^* \partial^\mu K D^\dagger \right), \\ \mathcal{L}_{\bar{D}_{s1} D K^*} &= g_{\bar{D}_{s1} D K^*} D_{s1}^\mu K_\mu^* D^\dagger, \end{aligned}$$

$$\begin{aligned}
\mathcal{L}_{D_s DK^*} &= ig_{D_s DK^*} D^\mu \partial_\mu D_s^\dagger K^{*\mu}, \\
\mathcal{L}_{D_{s0} DK} &= g_{D_{s0} DK} \partial^\mu D \partial_\mu K, \\
\mathcal{L}_{D_s^* DK_1} &= g_{D_s^* DK_1} DK_1^\mu D_{s\mu}^{*\dagger}, \\
\mathcal{L}_{D_{s0} DK_1} &= ig_{D_{s0} DK_1} D_{s0}^* \partial^\mu DK_{1\mu}, \\
\mathcal{L}_{D_s DK_0^*} &= g_{D_s DK_0^*} K_0^* \partial_\mu D_s \partial^\mu D, \\
\mathcal{L}_{D_{s1} DK_0^*} &= ig_{D_{s1} DK_0^*} DK_0^{*\mu} D_{s1\mu}^\dagger,
\end{aligned} \tag{58}$$

thus the transition matrix element can be obtained as

$$\begin{aligned}
\langle D(p') K(q) | D_s^*(p) \rangle &= ig_{D_s^* DK} \epsilon_{D_s^*} \cdot q, \\
\langle D(p') K^*(q) | D_{s1}(p) \rangle &= g_{D_{s1} DK^*} \epsilon_{K^*}^* \cdot \epsilon_{D_{s1}}, \\
\langle D(p') K^*(q) | D_s(p) \rangle &= ig_{D_s DK^*} \epsilon_{K^*} \cdot (p + p'), \\
\langle D(p') K(q) | D_{s0}(p) \rangle &= g_{D_{s0} DK} p' \cdot q, \\
\langle D(p') K_1(q) | D_s^*(p) \rangle &= g_{D_s^* DK_1} \epsilon_{D_s^*} \cdot \epsilon_{K_1}, \\
\langle D(p') K_1(q) | D_{s0}^*(p) \rangle &= ig_{D_{s0} DK_1} \epsilon_{K_1} \cdot p', \\
\langle D(p') K_0^*(q) | D_s(p) \rangle &= g_{D_s DK_0^*} p \cdot p', \\
\langle D(p') K_0^*(q) | D_{s1}(p) \rangle &= ig_{D_{s1} DK_0^*} \epsilon_{D_{s1}}^* \cdot q.
\end{aligned} \tag{59}$$

With the above coupling relations and transition matrix element, we can obtain the three-point correlator process on the phenomenological side. For $D_s^* DK$ process,

$$\begin{aligned}
\Pi_\mu(p, p', q) &= \int d^4x d^4y e^{ip' \cdot x} e^{iq \cdot y} \langle 0 | T \{ J_D(x) J_{K^0}(y) J_{D_s^*}^\dagger(0) \} | 0 \rangle \\
&= \frac{\lambda_{D_s^*} \lambda_D \lambda_K g_{D_s^* DK}}{(p'^2 - m_D^2)(p^2 - m_{D_s^*}^2)(q^2 - m_K^2)} \left(p'_\mu - \frac{m_{D_s^*}^2 + m_D^2 - q^2}{2m_{D_s^*}^2} p_\mu \right) + \dots
\end{aligned} \tag{60}$$

On the OPE side, we can evaluate the correlation function with the standard QCD sum rules approach. The related Feynman diagrams of the OPE series are shown in Fig. 6. To establish a sum rule for the coupling constant $g_{D_s^* DK}$, we will pick out the p_μ structure in the OPE series and then match both sides of the sum rule. After performing the double Borel transform $P^2 = -p^2 \rightarrow M_B^2, P'^2 = -p'^2 \rightarrow M_B'^2$ on both sides, we obtain

$$g_{D_s^* DK}(M_B^2, M_B'^2, Q^2) = -\frac{1}{4\pi^2} \frac{2m_{D_s^*}^2}{\lambda_{D_s^*} \lambda_D \lambda_K e^{-m_{D_s^*}^2/M_B^2 - m_D^2/M_B'^2}} \frac{Q^2 + m_K^2}{m_{D_s^*}^2 + m_D^2 + Q^2} \int_{m_c^2}^{s_0} ds \int_{m_c^2}^{u_0} du \rho(s, u, t) e^{-s/M_B^2 - u/M_B'^2}, \tag{61}$$

where

$$\rho(s, u, t) = -\frac{48\pi^4 t u (2m_c^2 - s + t - u)}{\lambda^{3/2}(s, u, t)} + \frac{2\pi^4 (s - t - 3u)}{3\lambda^{3/2}(s, u, t)} \langle GG \rangle, \tag{62}$$

and the Mandelstam invariances satisfy the relation:

$$(s - m_c^2)(u - m_c^2) \geq Q^2 m_c^2. \tag{63}$$

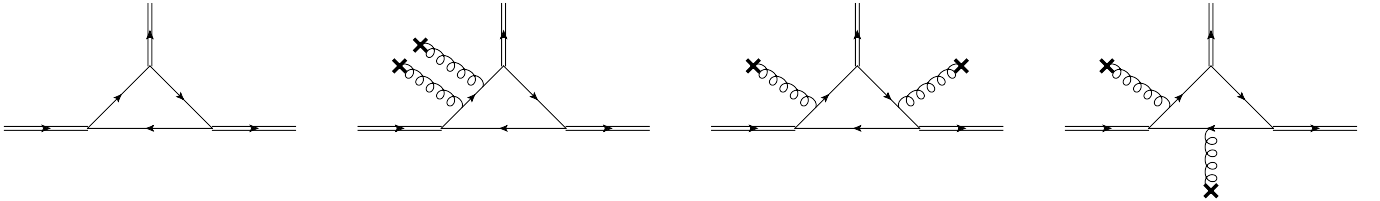


FIG. 6: The Feynman diagrams for OPE series of the correlation function (62). The double solid line denotes the in(out)-coming hadron, while the single solid line denotes the quark propagator. Diagrams related by symmetry are not shown.

To perform the numerical analysis, we use the following relation between the Borel masses which is proposed in Ref. [76]:

$$M_B'^2 = \frac{m_{\text{out}}^2}{m_{\text{in}}^2} M_B^2. \quad (64)$$

In this case, we shall use the relation as follow:

$$M_B'^2 = \frac{m_D^2}{m_{D_s^*}^2} M_B^2, \quad (65)$$

and the continuum threshold parameters is taken from Ref. [62]. To determine the proper Borel masses in our sum rule analysis, we define the pole contribution(PC) as

$$\text{PC}(Q^2) = \frac{\int_{m_c^2}^{s_0} ds' \int_{m_c^2}^{u_0} du' \rho(s', u', -Q^2) e^{-s'/M_B^2 - u'/M_B'^2}}{\int_{m_c^2}^{\infty} ds' \int_{m_c^2}^{\infty} du' \rho(s', u', -Q^2) e^{-s'/M_B^2 - u'/M_B'^2}} \quad (66)$$

and we ensure the PC at least at 40%. We show the PC for $g_{D_s^* DK}$ in the left panel of Fig. 7 and find that the proper M_B^2 should be 5.0 GeV^2 . We show the dependence of $g_{D_s^* DK}$ on Borel mass in the right panel of Fig. 7 and we can find a relatively steady platform around the chosen Borel mass, where we can obtain a stable result at $Q^2 = 3.5 \text{ GeV}^2 \sim m_D^2$. We fit our result from Q^2 range 3.5 to 4.0 GeV^2 with the exponential model:

$$g_{D_s^* DK}(Q^2) = (2.82^{+1.34}_{-0.82} \text{ GeV}^{-2}) e^{-(0.22 \pm 0.01 \text{ GeV}^{-2}) Q^2}, \quad (67)$$

which is shown in Fig. 8. The numerical analysis for coupling constants of other vertices is similar, we only list out their corresponding sum rules and spectrum functions in Appendix B and list out the results in Tab. III. The exponential fitting curves are also shown in Fig. 8.

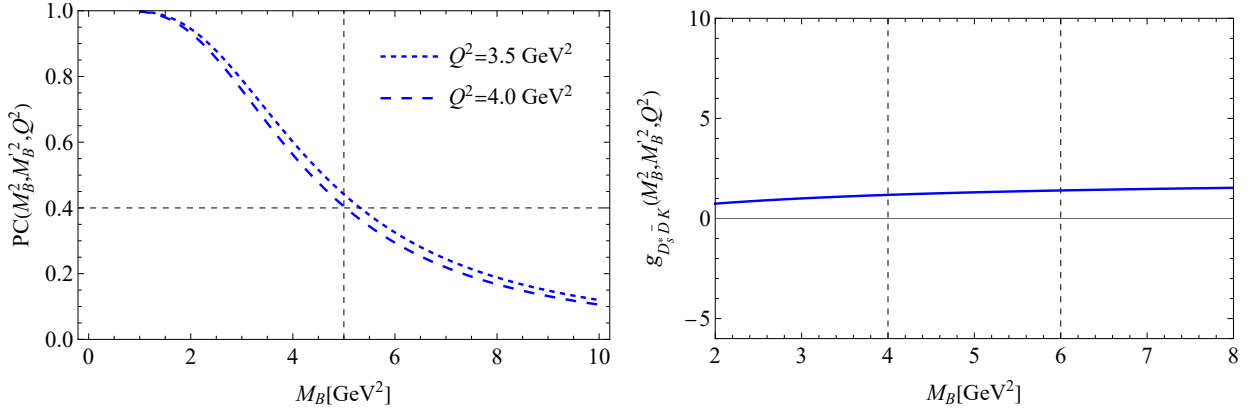


FIG. 7: The dependence of the pole contribution (left panel) and coupling $g_{D_s^* DK}$ (right panel) on the Borel mass M_B^2 . On the left panel, the transfer momentum is set to be $Q^2 = 3.5 \text{ GeV}^2$ (blue dotted curve) and $Q^2 = 4.0 \text{ GeV}^2$ (blue dashed curve), where the Q^2 region is chosen around m_D^2 and sufficient far away from m_K^2 to ensure the validity of sum rule. On the right panel, the coupling $g_{D_s^* DK}$ with $Q^2 = 3.5 \text{ GeV}^2$ behaves very stable around $M_B^2 = 5 \text{ GeV}^2$, with uncertainty estimated by the Borel mass uncertainty $\Delta M_B^2 = \pm 1 \text{ GeV}^2$

IV. DECAY AND PRODUCTION OF $X(2900)$

We obtain all the coupling constants in Eq. (11) and Eq. (13) in the above sections, in this section we shall obtain the branching fraction of the $B \rightarrow DX_0(2900)$ production process as well as the decay width of the $X_0(2900)$. The decay width of the two-body strong decay process $X_0(2900) \rightarrow \bar{D}K^0$ can be derived from Eq.(52) as

$$\Gamma(X_0(2900) \rightarrow \bar{D}^0 K^0) = \frac{\lambda^{1/2}(m_{X_0}^2, m_D^2, m_K^2)}{64\pi m_{X_0}} g_{\bar{D}KX_0}^2 (-m_K^2) (m_{X_0}^2 - m_D^2 - m_K^2)^2. \quad (68)$$

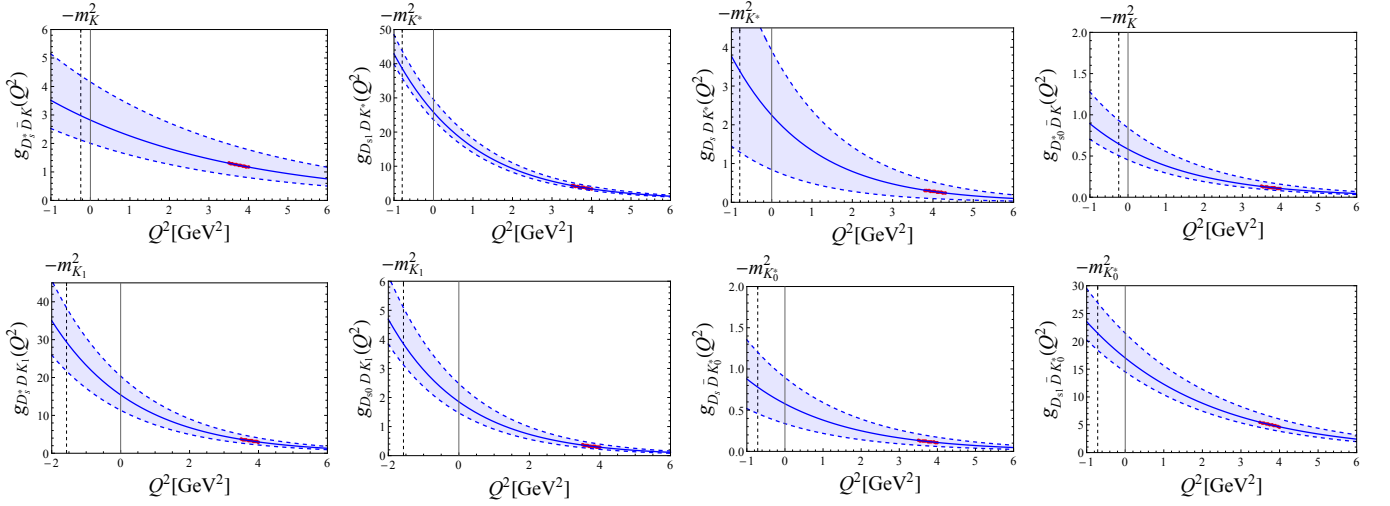


FIG. 8: The dependence of the coupling constant $g_{D_{s(1)}^* \bar{D} K^{(*)}}$ on the transfer momentum Q^2 , with Borel mass M_B^2 and continuum threshold s_0 listed in Tab. III. For each figure, the red dots denote the value from the corresponding sum rules while the blue solid line is the exponential fitting curve. The two dashed blue lines denote the upper and lower boundary of the uncertainty from the Borel masses, various condensates, quark masses and hadronic parameters.

TABLE III: Fitting coefficients with exponential model of coupling constants. The continuum thresholds s_0 are taken from Ref. [62]. The latter two columns shows the coupling constants with on-shell condition $Q^2 = -m_{K^{(*)}}^2$ in this work and other works.

	$M_B^2 [\text{GeV}^2]$	$s_0 [\text{GeV}^2]$	$a [\text{GeV}^2]$	$b [\text{GeV}^{-2}]$	g	Other Work
$g_{D_s^* DK}$	5.0	7.40	$2.82^{+1.34}_{-0.82}$	0.22 ± 0.00	$2.98^{+1.90}_{-1.61}$	2.84 ± 0.31 [77]
$g_{D_{s0}^* DK}$	8.6	6.84	$0.58^{+0.26}_{-0.13}$	0.43 ± 0.01	$0.65^{+0.29}_{-0.14}$	0.52 ± 0.17 [78]
$g_{D_{s1} DK^*}$	4.8	6.25	$25.81^{+6.60}_{-3.45}$	0.51 ± 0.01	$38.59^{+5.70}_{-3.66}$	$23.7 \sim 24.9$ [79]
$g_{D_s DK^*}$	5.0	6.30	$2.25^{+1.67}_{-1.41}$	$0.52^{+0.03}_{-0.02}$	$3.39^{+2.56}_{-2.19}$	2.85 ± 0.46 [80]
$g_{D_s^* DK_1}$	5.0	7.40	$15.41^{+4.96}_{-4.06}$	0.41 ± 0.00	$29.36^{+9.74}_{-7.84}$	11.92 ± 4.64 [81]
$g_{D_{s0}^* DK_1}$	5.2	6.84	$1.85^{+0.62}_{-0.39}$	0.46 ± 0.01	$3.84^{+1.32}_{-0.89}$	-
$g_{D_s DK_0^*}$	6.4	6.30	$0.58^{+0.32}_{-0.24}$	0.42 ± 0.01	$0.78^{+0.43}_{-0.33}$	0.74 ± 0.05 [82]
$g_{D_{s1} DK_0^*}$	5.0	6.25	$17.01^{+4.45}_{-2.50}$	0.33 ± 0.00	$21.45^{+5.66}_{-3.28}$	-

Then we can calculate the partial decay width of the process $X_0(2900) \rightarrow \bar{D}K^0$ as

$$\Gamma(X_0(2900) \rightarrow \bar{D}^0 K^0) = 32.03 \pm 9.12 \text{ MeV}, \quad (69)$$

where the error mainly comes from the uncertainties of the coupling constant $g_{\bar{D}KX_0}$. It should be noted that in our previous calculation in Sec. III, we adopt the light quark mass as $m_q = 0$, which would lead to the isospin symmetry $g_{\bar{D}^0 K^0 X_0} = g_{D^- K^+ X_0}$. Ignoring the small differences due to phase space, the total $\bar{D}K$ decay width should be

$$\begin{aligned} \Gamma(X_0(2900) \rightarrow \bar{D}K) &= \Gamma(X_0(2900) \rightarrow \bar{D}^0 K^0) + \Gamma(X_0(2900) \rightarrow D^- K^+) \\ &= 2\Gamma(X_0(2900) \rightarrow \bar{D}^0 K^0) \\ &= 64.07 \pm 18.23 \text{ MeV}. \end{aligned} \quad (70)$$

Due to the estimations that $X_0(2900)$ dominantly decay into $\bar{D}K$ channel [44, 45], our result is well consistent with the experimental result Eq.(1). The decay widths for other structures of $X_0(2900)$ are listed in Tab. V.

With the coupling constants obtained in Sec. III and the weak transition form factor is parametrized as [57]

$$F(Q^2) = \frac{F(0)}{1 - a(Q^2/m_B^2) + b(Q^2/m_B^2)^2}, \quad (71)$$

TABLE IV: The values of the parameters $F(0)$, a and b in the form factors Eq.(71) for $B \rightarrow D_{(0,1)}^{(*)}$ taken from Ref. [57].

Form Factor	$F(0)$	a	b	Form Factor	$F(0)$	a	b
$F_1^{B \rightarrow D}$	0.67	1.22	0.36	$F_1^{B \rightarrow D_0^*}$	0.24	1.03	0.27
$F_0^{B \rightarrow D}$	0.67	0.63	0.01	$F_0^{B \rightarrow D_0^*}$	0.24	-0.49	0.35
$A_0^{B \rightarrow D^*}$	0.68	1.21	0.36	$A_0^{B \rightarrow D_1}$	0.08	1.28	-0.29
$A_1^{B \rightarrow D^*}$	0.65	0.60	0.00	$A_1^{B \rightarrow D_1}$	-0.19	-1.25	0.97
$A_2^{B \rightarrow D^*}$	0.61	1.12	0.31	$A_2^{B \rightarrow D_1}$	-0.12	0.67	0.20
$A_V^{B \rightarrow D^*}$	0.77	1.25	0.38	$A_V^{B \rightarrow D_1}$	-0.12	0.71	0.18

TABLE V: Amplitudes for diagrams in Fig. 2, branch fraction and decay width for $X_0(2900)$ with molecule structure and tetraquark structure. The subscription indices a-h denote the corresponding diagrams in Fig. 2. The latter three columns denote the molecule structure, scalar-scalar compact structure and axialvector-axialvector structure correspondingly.

	mol	S-S	A-A
$\mathcal{A}_a [\times 10^{-8}]$	$-4.16^{+1.71}_{-2.50}$	$-2.97^{+1.35}_{-1.91}$	$-3.62^{+1.57}_{-2.26}$
$\mathcal{A}_b [\times 10^{-8}]$	$+3.67^{+0.78}_{-0.34}$	$+1.14^{+0.63}_{-0.31}$	$+1.08^{+0.62}_{-0.30}$
$\mathcal{A}_c [\times 10^{-8}]$	$+0.10^{+0.04}_{-0.05}$	$+0.03^{+0.03}_{-0.02}$	$+0.03^{+0.03}_{-0.02}$
$\mathcal{A}_d [\times 10^{-8}]$	$-4.33^{+0.81}_{-2.15}$	$-3.09^{+0.72}_{-1.67}$	$-3.77^{+0.80}_{-1.96}$
$\mathcal{A}_e [\times 10^{-8}]$	$-1.73^{+0.31}_{-0.43}$	$-0.45^{+0.08}_{-0.24}$	$-0.90^{+0.16}_{-0.35}$
$\mathcal{A}_f [\times 10^{-8}]$	$+0.02^{+0.01}_{-0.00}$	$+0.01^{+0.04}_{-0.00}$	$+0.01^{+0.05}_{-0.01}$
$\mathcal{A}_g [\times 10^{-8}]$	$-0.91^{+0.05}_{-0.02}$	$-0.13^{+0.09}_{-0.08}$	$-0.26^{+0.17}_{-0.14}$
$\mathcal{A}_h [\times 10^{-8}]$	$-0.57^{+0.07}_{-0.07}$	$-0.08^{+0.03}_{-0.03}$	$-0.16^{+0.05}_{-0.04}$
$Br(B^+ \rightarrow D^+ X_0) [\times 10^{-5}]$	$2.47^{+2.07}_{-1.55}$	$1.20^{+1.39}_{-0.80}$	$2.26^{+2.06}_{-1.33}$
$\Gamma(X_0 \rightarrow DK) [\text{MeV}]$	64.07 ± 18.23	32.49 ± 21.11	48.31 ± 21.78

the corresponding parameters are listed in Tab. IV, we can calculate the amplitude (11)-(20) as well as the decay width of the production process $B^+ \rightarrow D^+ X_0(2900)$ through

$$\Gamma(B^+ \rightarrow D^+ X_0) = \frac{\lambda^{1/2}(m_B^2, m_D^2, m_{X_0}^2)}{16\pi m_B^3} \left| \sum_{i=a}^h \mathcal{A}_i \right|^2, \quad (72)$$

and its corresponding branching fraction

$$Br(B^+ \rightarrow D^+ X_0) = \frac{\Gamma(B^+ \rightarrow D^+ X_0)}{\Gamma_{\text{tot}}}. \quad (73)$$

We list out the results in Tab. V.

V. DISCUSSION AND CONCLUSION

In this work, we mainly consider the branching fraction of the $X_0(2900)$ production process shown in Fig. 2 with different interpretation of $X_0(2900)$ state. By deriving the decay amplitudes of Fig. 2, we investigate the related strong decay vertices with QCD sum rule approach. The corresponding results are listed in Tab. V, from which one can see that the branching fraction and decay width of $X_0(2900)$ in the molecular picture are well consistent with the experimental results [22, 23], indicating that the $X_0(2900)$ state could be more likely a molecular state candidate. Such conclusion meets agreement with Ref. [33–41, 44, 45], where the decay width is calculated as $59.37^{+24.94}_{-17.96}$ MeV with effective Lagrangian formalism [44] and 49.6 ± 9.3 MeV with

light-cone QCD sum rule [39]. But we still cannot exclude the interpretation for axialvector-axialvector compact structure within the uncertainty. From Tab. V, we can see that the major contributions come from the $B^+ \rightarrow \bar{D}^0 D_s^{*+} \rightarrow D^+ X_0(2900)$, $B^+ \rightarrow \bar{D}^{*0} D_{s1}^+ \rightarrow D^+ X_0(2900)$ and $B^+ \rightarrow \bar{D}^0 D_{s0}^+ \rightarrow D^+ X_0(2900)$ processes, while the contribution from $B^+ \rightarrow \bar{D}^{*0} D_{s1}^+ \rightarrow D^+ X_0(2900)$ process in the molecular interpretation is much larger than that in the compact interpretations. It is because the coupling from $\bar{D}^* K^* X_0$ vertex in the molecular interpretation is much larger than that in the compact one. It is interesting to note that our branching fraction of the process $B^+ \rightarrow D^+ X \rightarrow D^+ (D^- K^+)$, $B^+ \rightarrow D^+ X \rightarrow D^+ (\bar{D}^0 K^0)$, $B^0 \rightarrow D^0 X \rightarrow D^0 (\bar{D}^0 K^0)$ and $B^0 \rightarrow D^0 X \rightarrow D^0 (D^- K^+)$ should be the same due to $\mathcal{B}r(B \rightarrow DX \rightarrow D\bar{D}K) = \mathcal{B}r(B \rightarrow DX)\mathcal{B}r(X \rightarrow \bar{D}K)$. In Ref. [46], the result shows that the branching fraction of process $B^+ \rightarrow D^+ X \rightarrow D^+ (\bar{D}^0 K^0)$ and $B^0 \rightarrow D^0 X \rightarrow D^0 (D^- K^+)$ would be highly suppressed with the triangle model. Future experimental studies can discriminate among the molecule, compact tetraquark or triangle singularity interpretations for the $X_0(2900)$ state.

ACKNOWLEDGMENTS

This work is partly supported by the National Natural Science Foundation of China with Grant Nos. 12375073, 12035007, and 12175318, Guangdong Provincial funding with Grant Nos. 2019QN01X172, Guangdong Major Project of Basic and Applied Basic Research No. 2020B0301030008, the Natural Science Foundation of Guangdong Province of China under Grant No. 2022A1515011922, the NSFC and the Deutsche Forschungsgemeinschaft (DFG, German Research Foundation) through the funds provided to the Sino-German Collaborative Research Center TRR110 ‘‘Symmetries and the Emergence of Structure in QCD’’ (NSFC Grant No. 12070131001, DFG Project-ID 196253076-TRR 110).

Appendix A: Spectrum function for three-point correlation of $D_{(0,1)}^{(*)} K_{(0,1)}^{(*)} X_0$ vertices

The spectrum function $\rho(s)$ and $R(M_B^2)$ in Eq.(42) with $\bar{D}^* K^*$ molecule structure is shown as follow

$$\rho(s) = \int_{x_{\min}}^1 dx \frac{m_c(1-x)}{8\pi^2} (\langle \bar{q}q \rangle + \langle \bar{s}s \rangle) + \int_0^1 dx \left(\frac{m_c m_s(x-1)}{256\pi^4} \langle GG \rangle - \frac{m_c x(x-1)}{32\pi^2} (\langle \bar{q}\sigma \cdot Gq \rangle + \langle \bar{s}\sigma \cdot Gs \rangle) \right), \quad (A1)$$

$$R(M_B^2) = -\frac{1}{96\pi^2 M_B^8} \left(2m_c^2 m_s \langle \bar{q}q \rangle \langle GG \rangle + \pi^2 M_B^6 \langle \bar{q}\sigma \cdot Gq \rangle (\langle \bar{q}q \rangle + \langle \bar{s}s \rangle) + 4M_B^4 \left(3m_s \langle \bar{q}\sigma \cdot Gq \rangle + 16\pi^2 \langle \bar{q}q \rangle (\langle \bar{q}q \rangle + \langle \bar{s}s \rangle) \right) \right. \\ \left. + 4M_B^2 m_c^2 \left(3m_s \langle \bar{q}\sigma \cdot Gq \rangle + 16\pi^2 \langle \bar{q}q \rangle (\langle \bar{q}q \rangle + \langle \bar{s}s \rangle) \right) \right), \quad (A2)$$

where $x_{\min} = 1 - m_c^2/s$ and $\Delta(s, x) = (1-x)(m_c^2 - sx)$, and in Eq.(47)

$$\rho(s) = \int_{x_{\min}}^1 dx \left(-\frac{2m_s \Delta(s, x) + m_s s(x-1)x}{4\pi^2} \langle \bar{q}q \rangle + \frac{m_s \Delta(s, x) + m_s s(x-1)x}{8\pi^2} \langle \bar{s}s \rangle \right. \\ \left. - \frac{3\Delta(s, x) + s(x-1)x}{384\pi^4} \langle GG \rangle - \frac{m_s x}{16\pi^2} (2\langle \bar{q}\sigma \cdot Gq \rangle + \langle \bar{s}\sigma \cdot Gs \rangle) \right) \\ + \int_0^1 dx \left(\frac{m_s s(1-x)x^2}{48\pi^2} (3\langle \bar{q}\sigma \cdot Gq \rangle + \langle \bar{s}\sigma \cdot Gs \rangle) + \frac{m_s(x-1)x}{192\pi^2} \langle GG \rangle (\langle \bar{s}s \rangle - 3\langle \bar{q}q \rangle) \right), \quad (A3)$$

$$R(M_B^2) = -\frac{1}{96\pi^2 M_B^6} \left(4m_c^3 \langle \bar{q}q \rangle \langle GG \rangle + \pi^2 m_c m_s (4\langle \bar{q}q \rangle - \langle \bar{s}s \rangle) (M_B^4 \langle \bar{q}\sigma \cdot Gq \rangle + 64m_c^2 \langle \bar{q}q \rangle) \right), \quad (A4)$$

and in Eq.(54)

$$\rho(s) = \int_{x_{\min}}^1 dx \left(-\frac{2m_s \Delta(s, x) + m_s s(x-1)x}{4\pi^2} \langle \bar{q}q \rangle + \frac{m_s \Delta(s, x) + m_s s(x-1)x}{8\pi^2} \langle \bar{s}s \rangle \right. \\ \left. - \frac{3\Delta(s, x) + s(x-1)x}{384\pi^4} \langle GG \rangle + \frac{m_s x}{16\pi^2} (2\langle \bar{q}\sigma \cdot Gq \rangle - \langle \bar{s}\sigma \cdot Gs \rangle) \right) \\ + \int_0^1 dx \left(\frac{m_s s(1-x)x^2}{48\pi^2} (3\langle \bar{q}\sigma \cdot Gq \rangle - \langle \bar{s}\sigma \cdot Gs \rangle) + \frac{m_s(x-1)x}{192\pi^2} \langle GG \rangle (\langle \bar{s}s \rangle + 4\langle \bar{q}q \rangle) \right), \quad (A5)$$

$$R(M_B^2) = \frac{1}{96\pi^2 M_B^6} \left(4m_c^3 \langle \bar{q}q \rangle \langle GG \rangle - \pi^2 m_c m_s (4\langle \bar{q}q \rangle + \langle \bar{s}s \rangle) (M_B^4 \langle \bar{q}\sigma \cdot Gq \rangle + 64m_c^2 \langle \bar{q}q \rangle) \right), \quad (A6)$$

and in Eq.(55)

$$\rho(s) = \int_{x_{\min}}^1 dx \frac{m_c(1-x)}{8\pi^2} (\langle \bar{s}s \rangle - \langle \bar{q}q \rangle) - \int_0^1 dx \left(\frac{m_c(1-x)x}{32\pi^2} (\langle \bar{q}\sigma \cdot Gq \rangle + \langle \bar{s}\sigma \cdot Gs \rangle) + \frac{m_c m_s(1-x)}{256\pi^4} \langle GG \rangle \right), \quad (A7)$$

$$R(M_B^2) = \frac{1}{96\pi^2 M_B^8} \left(2m_c^2 m_s \langle \bar{q}q \rangle \langle GG \rangle + \pi^2 M_B^6 \langle \bar{q}\sigma \cdot Gq \rangle (\langle \bar{s}s \rangle - \langle \bar{q}q \rangle) + 4M_B^4 (3m_s \langle \bar{q}\sigma \cdot Gq \rangle + 16\pi^2 \langle \bar{q}q \rangle (\langle \bar{s}s \rangle - \langle \bar{q}q \rangle)) \right. \\ \left. + 4M_B^2 m_c^2 (3m_s \langle \bar{q}\sigma \cdot Gq \rangle + 16\pi^2 \langle \bar{q}q \rangle (\langle \bar{s}s \rangle - \langle \bar{q}q \rangle)) \right). \quad (A8)$$

The spectrum function $\rho(s)$ and $R(M_B^2)$ in Eq.(42) with scalar-diquark-scalar-antidiquark structure is shown as follow

$$\rho(s) = \int_{x_{\min}}^1 dx \frac{m_c(1-x)}{8\pi^2} (\langle \bar{q}q \rangle + \langle \bar{s}s \rangle), \quad (A9)$$

$$R(M_B^2) = -\frac{1}{96M_B^6} (\langle \bar{q}q \rangle + \langle \bar{s}s \rangle) (M_B^2 \langle \bar{q}\sigma \cdot Gq \rangle + 64 \langle \bar{q}q \rangle (M_B^2 + m_c^2)), \quad (A10)$$

and in Eq.(47)

$$\rho(s) = \int_{x_{\min}}^1 dx \left(\frac{2m_s(\Delta(s, x) + s(x-1)x)}{4\pi^2} \langle \bar{q}q \rangle - \frac{m_s(\Delta(s, x) + s(x-1)x)}{8\pi^2} \langle \bar{s}s \rangle + \frac{3\Delta(s, x) + s(x-1)x}{384\pi^4} \langle GG \rangle \right) \\ + \int_0^1 dx \left(\frac{m_s(x-1)x}{192\pi^2} \langle \bar{s}s \rangle \langle GG \rangle - \frac{m_s(x-1)x}{48\pi^2} \langle \bar{q}q \rangle \langle GG \rangle \right), \quad (A11)$$

$$R(M_B^2) = \frac{1}{96\pi^2 M_B^6} (4m_c^3 \langle \bar{q}q \rangle \langle GG \rangle + \pi^2 m_c m_s (4 \langle \bar{q}q \rangle - \langle \bar{s}s \rangle) (M_B^4 \langle \bar{q}\sigma \cdot Gq \rangle + 64m_c^2 \langle \bar{q}q \rangle)), \quad (A12)$$

and in Eq.(54)

$$\rho(s) = \int_{x_{\min}}^1 dx \left(\frac{2m_s \Delta(s, x) + m_s s(x-1)x}{4\pi^2} \langle \bar{q}q \rangle + \frac{m_s \Delta(s, x) + m_s s(x-1)x}{8\pi^2} \langle \bar{s}s \rangle - \frac{3\Delta(s, x) + s(x-1)x}{384\pi^4} \langle GG \rangle \right) \\ + \int_0^1 dx \frac{m_s(1-x)x^2}{192\pi^2} (4 \langle \bar{q}q \rangle + \langle \bar{s}s \rangle) \langle GG \rangle, \quad (A13)$$

$$R(M_B^2) = \frac{1}{96\pi^2 M_B^6} (4m_c^3 \langle \bar{q}q \rangle \langle GG \rangle - \pi^2 m_c m_s (4 \langle \bar{q}q \rangle + \langle \bar{s}s \rangle) (M_B^4 \langle \bar{q}\sigma \cdot Gq \rangle + 64m_c^2 \langle \bar{q}q \rangle)), \quad (A14)$$

and in Eq.(55)

$$\rho(s) = \int_{x_{\min}}^1 dx \frac{m_c(1-x)}{8\pi^2} (\langle \bar{s}s \rangle - \langle \bar{q}q \rangle) \quad (A15)$$

$$R(M_B^2) = -\frac{1}{96M_B^6} (\langle \bar{q}q \rangle - \langle \bar{s}s \rangle) (M_B^4 \langle \bar{q}\sigma \cdot Gq \rangle + 64 \langle \bar{q}q \rangle (M_B^2 + m_c^2)). \quad (A16)$$

The spectrum function $\rho(s)$ and $R(M_B^2)$ in Eq.(42) with axialvector-diquark-axialvector-antidiquark structure is shown as follow

$$\rho(s) = \int_{x_{\min}}^1 dx \frac{m_c(x-1)}{4\pi^2} (\langle \bar{q}q \rangle + \langle \bar{s}s \rangle), \quad (A17)$$

$$R(M_B^2) = \frac{1}{48M_B^6} (\langle \bar{q}q \rangle + \langle \bar{s}s \rangle) (64(M_B^2 + m_c^2) \langle \bar{q}q \rangle + M_B^4 \langle \bar{q}\sigma \cdot Gq \rangle), \quad (A18)$$

and in Eq.(47)

$$\rho(s) = \int_{x_{\min}}^1 dx \left(\frac{2m_s \Delta(s, x) + m_s s(x-1)x}{2\pi^2} \langle \bar{q}q \rangle - \frac{m_s \Delta(s, x) + m_s s(x-1)x}{4\pi^2} \langle \bar{s}s \rangle + \frac{3\Delta(s, x) + s(x-1)x}{192\pi^4} \langle GG \rangle \right) \\ + \int_0^1 dx \frac{m_s(x-1)x}{24\pi^2} \langle GG \rangle (\langle \bar{s}s \rangle - 4 \langle \bar{q}q \rangle), \quad (A19)$$

$$R(M_B^2) = \frac{1}{48\pi^2 M_B^6} \left(4m_c^3 \langle \bar{q}q \rangle \langle GG \rangle + \pi^2 m_c m_s (4\langle \bar{q}q \rangle - \langle \bar{s}s \rangle) \left(M_B^4 \langle \bar{q}\sigma \cdot Gq \rangle + 64m_c^2 \langle \bar{q}q \rangle \right) \right), \quad (\text{A20})$$

and in Eq.(54)

$$\begin{aligned} \rho(s) = & \int_{x_{\min}}^1 dx \left(-\frac{2m_s \Delta(s, x) + m_s s(x-1)x}{2\pi^2} \langle \bar{q}q \rangle - \frac{m_s \Delta(s, x) + m_s s(x-1)x}{4\pi^2} \langle \bar{s}s \rangle + \frac{3\Delta(s, x) + s(x-1)x}{192\pi^4} \langle GG \rangle \right) \\ & - \int_0^1 dx \frac{m_s(1-x)x}{96\pi^2} (4\langle \bar{q}q \rangle + \langle \bar{s}s \rangle) \langle GG \rangle, \end{aligned} \quad (\text{A21})$$

$$R(M_B^2) = \frac{1}{48\pi^2 M_B^6} \left(-4m_c^3 \langle \bar{q}q \rangle \langle GG \rangle + \pi^2 m_c m_s (4\langle \bar{q}q \rangle + \langle \bar{s}s \rangle) (M_B^4 \langle \bar{q}\sigma \cdot Gq \rangle + 64m_c^2 \langle \bar{q}q \rangle) \right), \quad (\text{A22})$$

and in Eq.(55)

$$\rho(s) = \int_{x_{\min}}^1 dx \frac{m_c(x-1)}{4\pi^2} (\langle \bar{s}s \rangle - \langle \bar{q}q \rangle) \quad (\text{A23})$$

$$R(M_B^2) = -\frac{1}{48M_B^6} (\langle \bar{q}q \rangle - \langle \bar{s}s \rangle) \left(M_B^4 \langle \bar{q}\sigma \cdot Gq \rangle + 64\langle \bar{q}q \rangle (M_B^2 + m_c^2) \right), \quad (\text{A24})$$

Appendix B: Sum rule for three-point correlation of $D_{s(0,1)}^{(*)} DK_{(0,1)}^{(*)}$ vertices

For $D_{s1} DK^*$ process, the sum rule can be obtained as

$$g_{D_{s1} DK^*}(M_B^2, M_B'^2, Q^2) = -\frac{1}{4\pi^2} \frac{4m_{D_{s1}}^2 m_{K^*}^2}{\lambda_{D_{s1}} \lambda_D \lambda_{K^*} e^{-m_{D_{s1}}^2/M_B^2 - m_D^2/M_B'^2}} \frac{Q^2 + m_K^2}{\lambda(m_D^2, m_{D_{s1}}^2, -Q^2) + 12m_{D_{s1}}^2 m_{K^*}^2} \int_{m_c^2}^{s_0} ds' \int_{m_c^2}^{u_0} du' \rho(s', u', t) e^{-s'/M_B^2 - u'/M_B'^2}, \quad (\text{B1})$$

where

$$\rho(s, u, t) = \frac{48\pi^4 (2m_c^2 m_s - m_c(s+u) - 2m_s u)}{\lambda^{1/2}(s, u, t)}. \quad (\text{B2})$$

For $D_{s0}^* DK$ process, the sum rule can be obtained as

$$g_{D_{s0}^* DK}(M_B^2, M_B'^2, Q^2) = -\frac{1}{4\pi^2} \frac{1}{\lambda_{D_{s0}} \lambda_D \lambda_K e^{-m_{D_{s0}}^2/M_B^2 - m_D^2/M_B'^2}} \frac{2(Q^2 + m_K^2)}{m_{D_{s0}}^2 - m_D^2 + Q^2} \int_{m_c^2}^{s_0} ds' \int_{m_c^2}^{u_0} du' \rho(s', u', t) e^{-s'/M_B^2 - u'/M_B'^2}, \quad (\text{B3})$$

where

$$\begin{aligned} \rho(s, u, t) = & -\frac{48\pi^4}{\lambda^{5/2}(s, u, t)} \left(2m_c^3 (m_c(m_c + m_s) - s + t - u) (\lambda(s, u, t) + 3t(s - t + u)) + m_s u (s - t + u) \lambda(s, u, t) \right. \\ & - m_c^2 m_s (s(s^2 + s(t+u) - 5(t-u)^2) + 3(t-u)^2(t+u)) + m_c (s^2(s^2 - (s-t-u)(3t+2u) - s(t-u)(t^2 + 3tu - 2u^2) \\ & \left. - u(t-u)^3) + 6m_s stu(s-t+u) \right) - \frac{24\pi^4 \langle GG \rangle m_c (s(t-2u) + t(u-t))}{\lambda^{5/2}(s, u, t)}. \end{aligned} \quad (\text{B4})$$

For $D_s DK^*$ process, the sum rule can be obtained as

$$g_{D_s DK^*}(M_B^2, M_B'^2, Q^2) = -\frac{1}{4\pi^2} \frac{m_{K^*}^2}{\lambda_{D_s} \lambda_D \lambda_{K^*} e^{-m_{D_s}^2/M_B^2 - m_D^2/M_B'^2}} \frac{Q^2 + m_{K^*}^2}{m_{D_s}^2 - m_D^2 - m_{K^*}^2} \int_{m_c^2}^{s_0} ds' \int_{m_c^2}^{u_0} du' \rho(s', u', t) e^{-s'/M_B^2 - u'/M_B'^2}, \quad (\text{B5})$$

where

$$\rho(s, u, t) = -\frac{48\pi^4 (s-t-u)(m_c^4 - m_c^2(s-t+u) + su)}{\lambda^{3/2}(s, u, t)} + \frac{2\pi^4 \langle GG \rangle (s-t-u)}{3\lambda^{3/2}(s, u, t)} \quad (\text{B6})$$

For $D_s^* DK_1$ process, the sum rule can be obtained as

$$g_{D_s^* DK_1}(M_B^2, M_B'^2, Q^2) = -\frac{1}{4\pi^2} \frac{4m_{D_s^*}^2 m_{K_1}^2}{\lambda_{D_s^*} \lambda_D \lambda_{K_1} e^{-m_{D_s^*}^2/M_B^2 - m_D^2/M_B'^2}} \frac{Q^2 + m_K^2}{\lambda(m_{D_s^*}^2, m_{D_s}^2, -Q^2) + 12m_{D_s}^2 m_{K_1}^2} \int_{m_c^2}^{s_0} ds' \int_{m_c^2}^{u_0} du' \rho(s', u', t) e^{-s'/M_B^2 - u'/M_B'^2}, \quad (B7)$$

where

$$\rho(s, u, t) = -\frac{48\pi^4(2m_c^2 m_s + m_c(s+u) - 2m_s u)}{\sqrt{\lambda(s, u, t)}}. \quad (B8)$$

For $D_{s0}^* DK_1$ process, the sum rule can be obtained as

$$g_{D_{s0}^* DK_1}(M_B^2, M_B'^2, Q^2) = -\frac{1}{4\pi^2} \frac{1}{\lambda_{D_{s0}^*} \lambda_D \lambda_{K_1} e^{-m_{D_{s0}^*}^2/M_B^2 - m_D^2/M_B'^2}} (Q^2 + m_K^2) \int_{m_c^2}^{s_0} ds' \int_{m_c^2}^{u_0} du' \rho(s', u', t) e^{-s'/M_B^2 - u'/M_B'^2}, \quad (B9)$$

where

$$\rho(s, u, t) = -\frac{96\pi^4 t(m_c^4 - m_c^2(s-t+u) + su)}{\lambda^{3/2} + (s, u, t)} + \frac{4\pi^4 \langle GG \rangle t}{3\lambda^{3/2}(s, u, t)}. \quad (B10)$$

For $D_s DK_0^*$ process, the sum rule can be obtained as

$$g_{D_s DK_0^*}(M_B^2, M_B'^2, Q^2) = -\frac{1}{4\pi^2} \frac{2}{\lambda_{D_s} \lambda_D \lambda_{K_0^*} e^{-m_{D_s}^2/M_B^2 - m_D^2/M_B'^2}} \frac{Q^2 + m_{K_0^*}^2}{m_{D_s}^2 + m_D^2 + Q^2} \int_{m_c^2}^{s_0} ds' \int_{m_c^2}^{u_0} du' \rho(s', u', t) e^{-s'/M_B^2 - u'/M_B'^2}, \quad (B11)$$

where

$$\begin{aligned} \rho(s, u, t) = & \frac{48\pi^4}{\lambda^{5/2}(s, u, t)} \left(2m_c^3(\lambda(s, u, t) + 3t(s-t+u))(m_c^2 - m_c m_s - s + t - u) - m_s u(s-t+u)(\lambda(s, u, t) + 6st) \right. \\ & + m_c(m_c m_s(s^3 + s^2(t+u) - 5s(t-u)^2 + 3(t-u)^2(t+u)) - u(s(s-2t)(2s-t) + t^3) - u^2(2s+3t)(s+t-u) \\ & \left. + s(s-t)^3 + u^4) \right) + \frac{24\pi^4 \langle GG \rangle m_c(s(t-2u) + t(u-t))}{\lambda^{5/2}(s, u, t)}. \end{aligned} \quad (B12)$$

For $D_{s1} DK_0^*$ process, the sum rule can be obtained as

$$g_{D_{s1} DK_0^*}(M_B^2, M_B'^2, Q^2) = -\frac{1}{4\pi^2} \frac{2m_{D_{s1}}^2}{\lambda_{D_{s1}} \lambda_D \lambda_{K_0^*} e^{-m_{D_{s1}}^2/M_B^2 - m_D^2/M_B'^2}} \frac{Q^2 + m_{K_0^*}^2}{m_{D_{s1}}^2 + m_D^2 + Q^2} \int_{m_c^2}^{s_0} ds' \int_{m_c^2}^{u_0} du' \rho(s', u', t) e^{-s'/M_B^2 - u'/M_B'^2}, \quad (B13)$$

where

$$\rho(s, u, t) = -\frac{48\pi^4 t u (2m_c^2 - s + t - u)}{\lambda^{3/2}(s, u, t)} + \frac{2\pi^4 \langle GG \rangle (s - t - 3u)}{3\lambda^{3/2}(s, u, t)}. \quad (B14)$$

-
- [1] M. Gell-Mann, Phys. Lett. **8**, 214 (1964)
[2] G. Zweig, in: D.Lichtenberg, S.P.Rosen(Eds.), Developments in the Quark Theory of Hadrons, VOL. 1. 1964 - 1978:pp. 22–101, 1964.
[3] R. L. Workman *et al.* [Particle Data Group], PTEP **2022**, 083C01 (2022)
[4] M. Nielsen, F.S. Navarra, S.H. and Lee, Phys. Rept. **497**, 41 (2010)
[5] H. X. Chen, W. Chen, X. Liu and S. L. Zhu, Phys. Rept. **639**, 1-121 (2016)
[6] J.-M. Richard, Few Body Syst. **57**, 1185 (2016)
[7] A. Esposito, A. Pilloni and A. D. Polosa, Phys. Rept. **668**, 1-97 (2017)
[8] A. Ali, J.S. Lange, and S. Stone, Prog. Part. Nucl. Phys. **97**, 123 (2017)
[9] F. K. Guo, C. Hanhart, U. G. Meißner, Q. Wang, Q. Zhao and B. S. Zou, Rev. Mod. Phys. **90**, no.1, 015004 (2018)
[10] R.M. Albuquerque, J.M. Dias, K.P. Khemchandani, A.M. Torres, F.S. Navarra, M. Nielsen, and C.M. Zanetti, J. Phys. G **46**, 093002 (2019)
[11] Y. R. Liu, H. X. Chen, W. Chen, X. Liu and S. L. Zhu, Prog. Part. Nucl. Phys. **107**, 237-320 (2019)

- [12] N. Brambilla, S. Eidelman, C. Hanhart, A. Nefediev, C. P. Shen, C. E. Thomas, A. Vairo and C. Z. Yuan, Phys. Rept. **873**, 1-154 (2020)
- [13] J.-M. Richard, A. Valcarce, and J. Vijande, Annals Phys. **412**, 168009 (2020)
- [14] R.N. Faustov, V.O. Galkin, and E.M. Savchenko, Universe **7**, 94 (2021)
- [15] H. X. Chen, W. Chen, X. Liu, Y. R. Liu and S. L. Zhu, Rept. Prog. Phys. **86**, 026201 (2023)
- [16] L. Meng, B. Wang, G. J. Wang and S. L. Zhu, Phys.Rept. **1019**, 1-149 (2023)
- [17] V. M. Abazov *et al.*[D0], Phys. Rev. Lett. **117**, no.2, 022003 (2016)
- [18] R. Aaij *et al.*[LHCb], Phys. Rev. Lett. **117** no.15, 152003 (2016)[Addendum: Phys. Rev. Lett. **118**, no.10, 109904 (2017)]
- [19] A. M. Sirunyan *et al.*[CMS], Phys. Rev. Lett. **120**, no.20, 202005 (2018)
- [20] T. Aaltonen *et al.*[CDF], Phys. Rev. Lett. **120**, no.20, 202006 (2018)
- [21] M.Aaboud *et al.*[ATLAS], Phys. Rev. Lett. **120**, no.20, 202007 (2018)
- [22] R. Aaij *et al.*[LHCb], Phys. Rev. Lett. **125**, 242001 (2020)
- [23] R. Aaij *et al.*[LHCb], Phys. Rev. D **102**, 112003 (2020)
- [24] Z. Yu, Q. Wu, and D.-Y. Chen, arXiv: 2310.12398 [hep-ph]
- [25] J.-B. Cheng, S.-Y. Li, Y.-R. Liu, Y.-N. Liu, Z.-G. Si, and T. Yao, Phys. Rev. D **101**, no.11, 114017 (2020)
- [26] T. Guo, J. Li, J. Zhao, and L. He, Phys. Rev. D **105**, 054018 (2022)
- [27] X.-G. He, W. Wang, and R. Zhu, Eur. Phys. J. C **80**, no.11, 1026 (2020)
- [28] G.-J. Wang, L. Meng, L.-Y. Xiao, M. Oka, and S.-L. Zhu, Eur. Phys. J. C **81**, no.2, 188 (2021)
- [29] J.-R. Zhang, Phys. Rev. D **103**, no.5, 054019 (2021)
- [30] Z.-G. Wang, Int. J. Mod. Phys. A **35**, no.30, 2050187 (2020)
- [31] Q.-F. Lü, D.-Y. Chen, and Y.-B. Dong, Phys. Rev. D **102**, no.7, 074021 (2020)
- [32] S.S. Agaev, K. Azizi, and H. Sundu, Phys. Rev. D **106**, no.1, 014019 (2022)
- [33] M.-W. Hu, X.-Y. Lao, P. Ling, and Q. Wang, Chin. Phys. C **45**, no.2, 021003 (2021)
- [34] S.-Y. Kong, J.-T. Zhu, D. Song, and J. He, Phys. Rev. D **104** no.9, 094012 (2021)
- [35] H.-W. Ke, Y.-F. Shi, X.-H. Liu, and X.-Q. Li, Phys. Rev. D **106**, no.11, 114032 (2022)
- [36] M.-Z. Liu, J.-J. Xie, L.-S. Geng, Phys. Rev. D **102**, no.9, 091502 (2020)
- [37] B. Wang, and S.-L. Zhu, Eur. Phys. J. C **82**, no.5, 419 (2022)
- [38] H.-X. Chen, W. Chen, R.-R. Dong, and N. Su, Chin. Phys. Lett. **37**, no.10, 101201 (2020)
- [39] S.S. Agaev, K. Azizi, and H. Sundu, J. Phys. G **48**, no.8, 085012 (2021)
- [40] H.-X. Chen, Phys. Rev. D **105**, no.9, 094003 (2022)
- [41] H. Mutuk, J. Phys. G **48**, no.5, 055007 (2021)
- [42] R. Molina, T. Branz, and E. Oset, Phys. Rev. D **82**, 014010 (2010)
- [43] R. Molina and E. Oset, Phys. Lett. B **811**, 135870 (2020) [Erratum: Phys. Lett. B **837**, 137645 (2023)]
- [44] Y. Huang, J.-X. Lu, J.-J. Xie, and L.-S. Geng, Eur. Phys. J. C **80**, no.10, 973 (2020)
- [45] C.-J. Xiao, D.-Y. Chen, Y.-B. Dong, and G.-W. Meng, Phys. Rev. D **103**, no.3, 034004 (2021)
- [46] T. J. Burns, and E. S. Swanson, Phys. Rev. D **103**, no.1, 014004 (2021)
- [47] T. J. Burns, and E. S. Swanson, Phys. Lett. B **813**, 136057 (2021)
- [48] Y.-K. Chen, J.-J. Han, Q.-F. Lü, J.-P. Wang, and F.-S. Yu, Eur. Phys. J. C **81**, no.1, 71 (2021)
- [49] Y.-K. Hsiao, and Y. Yu, Phys. Rev. D **104**, no.3, 034008 (2021)
- [50] J.-W. Li, M.-Z. Yang, and D.-S. Du, HEPNP **27**, 665-672 (2003)
- [51] H.-Y. Cheng, C.-K. Chua, and A. Soni, Phys. Rev. D **71**, 014030 (2005)
- [52] C.-D. Lü, Y.-L. Shen, and W. Wang, Phys. Rev. D **73**, 034005 (2006)
- [53] M. Wirbel, B. Stech, and M. Bauer, Z. Phys. C **29**, 637 (1985)
- [54] M. Bauer, B. Stech, and M. Wirbel, Z. Phys. C **34**, 103 (1987)
- [55] G. Buchalla, A.J. Buras, and M.E. Lautenbacher, Rev. Mod. Phys. **68**, 1125-1144 (1996)
- [56] O. Gortchakov, M.P. Locher, V.E. Markushin, and S. von Rotz, Z. Phys. A **353**, 447 (1996)
- [57] H.-Y. Cheng, C.-K. Chua, and C.-W. Hwang, Phys. Rev. D **69**, 074025 (2004)
- [58] L. J. Reinders, H. Rubinstein, and S. Yazaki, Phys. Rep. **127**, 1 (1985)
- [59] M. A. Shifman, A. I. Vainshtein, and V. I. Zakharov, Nucl. Phys. B **147**, 385 (1979)
- [60] P. Colangelo and A. Khodjamirian, *At the Frontier of Particle Physics*, edited by M. Shifman (World Scientific, Singapore, 2001), Vol. **3**, pp. 1495–1576
- [61] S. Narison, Camb. Monogr. Part. Phys. Nucl. Phys. Cosmol. **17**, 1-812 (2007) Cambridge University Press, 2022, ISBN 978-1-00-929029-6, 978-1-00-929031-9, 978-1-00-929033-3, 978-0-521-03731-0, 978-0-521-81164-4, 978-0-511-18948-7
- [62] P. Gelhausen, A. Khodjamirian, A.A. Pivovarov, and D. Rosenthal, Phys. Rev. D **88**, 014015 (2013) [Erratum: Phys. Rev. D **91**, 099901 (2015)]
- [63] N. Gubernari, A. Khodjamirian, R. Mandal, and T. Mannel, JHEP **12**, 015 (2023)
- [64] G. 't Hooft, G. Isidori, L. Maiani, A. D. Polosa, and V. Riquer, Phys. Lett. B **662**, 424 (2008)
- [65] S. Narison, QCD spectral sum rules, volume **26** (1989)
- [66] M. Jamin, J. A. Oller, and A. Pich, Eur. Phys. J. C **24**, 237 (2002)
- [67] M. Jamin and A. Pich, Nucl. Phys. B Proc. Suppl. **74**, 300 (1999)
- [68] B. L. Ioffe, Nucl. Phys. B **188**, 317 (1981), [Erratum: Nucl.Phys.B **191**, 591–592 (1981)]
- [69] Y. Chung, H. G. Dosch, M. Kremer, and D. Schall, Z. Phys. C **25**, 151 (1984)
- [70] H. G. Dosch, M. Jamin, and S. Narison, Phys. Lett. B **220**, 251 (1989)
- [71] A. Khodjamirian, T. Mannel, N. Offen, and Y. M. Wang, Phys. Rev. D **83**, 094031 (2011)
- [72] A. Francis, R. J. Hudspith, R. Lewis, and K. Maltman, Phys. Rev. D **99**, 054505 (2019)

- [73] R. Casalbuoni, A. Deandrea, N. Di Bartolomeo, R. Gatto, F. Feruglio and G. Nardulli, Phys. Rept. **281**, 145 (1997)
- [74] R. Casalbuoni, A. Deandrea, N. Di Bartolomeo, R. Gatto, F. Feruglio and G. Nardulli, Phys. Lett. B **292**, 371 (1992)
- [75] R. Casalbuoni, A. Deandrea, N. Di Bartolomeo, R. Gatto, F. Feruglio and G. Nardulli, Phys. Lett. B **299**, 139 (1993)
- [76] F.S. Navarra, M. Nielsen, M.E. Bracco, M. Chiapparini, and C.L. Schat, Phys. Lett. B **489**, 319 (2000)
- [77] M.E. Bracco, A. Cerqueira Jr., M. Chiapparini, A. Lozéa, and M. Nielsen, Phys. Lett. **B 641**, 286 (2006)
- [78] P. Colangelo, F. De Fazio, G. Nardulli, N. Di Bartolomeo, and R. Gatto, Phys. Rev. D **52**, 6422 (1995)
- [79] J.-X. Lin, H.-X. Chen, W.-H. Liang, C.-W. Xiao, and E. Oset, Eur. Phys. J. C **84**, no.4, 439 (2024)
- [80] M. Janbazi and R. Khosravi, Eur. Phys. J. C **78**, no.7, 606 (2018)
- [81] S. Momeni and R. Khosravi, arXiv: 2003.04165
- [82] H. Sundu, J.Y. Sungu, S. Sahin, N. Yinelek, and K. Azizi, Phys. Rev. D **83**, 114009 (2011)